SKI Report 91:9

Some Aspects of Regional Flow of Variable-Density Groundwater in Crystalline Basement Rock of Sweden

Clifford I. Voss
Johan Andersson

December 1991

ISSN 1104–1374
ISRN SKI-R-91/9-SE

SKI

Some Aspects of Regional Flow of Variable-Density Groundwater in Crystalline Basement Rock of Sweden

SKI TR 91:9

Clifford I. Voss
U.S. Geological Survey
431 National Center
Reston, Virginia 22092 USA
and
Johan Andersson
SKI
Box 27106
S-102 52 Stockholm, Sweden

December 1991

gotab 96521, Stockholm 1992

SOME ASPECTS OF REGIONAL FLOW OF VARIABLE-DENSITY GROUNDWATER IN CRYSTALLINE BASEMENT ROCK OF SWEDEN

Clifford I. Voss
U.S. Geological Survey
Reston, Virginia, USA and
Johan Andersson
Swedish Nuclear Power Inspectorate
Stockholm, Sweden

Abstract

The distribution of saltwaters in the Baltic Shield in Sweden is consistent with ongoing but incomplete Holocene flushing and depends on the geometry and connectivity of conductive structures at both regional and local scales, and on the surface topography. Numerical simulation of regional variable-density fluid flow during Holocene land-rise and coastal regression shows that the existence of any old saltwater, whether derived from submarine recharge in regions below Sweden's highest post-glacial coastline or geochemical processes, is an indication either of slow fluid movements through the bedrock over long times, or of long travel distances through fracture systems before arriving at measurement points. During the land-rise period, regional flow is not affected by the variable density of fluids in the upper few kilometers of the shield and the topography of the water table is the only driving force. The spatial distribution of meteoric flushing water and pre-Holocene waters may be complex, with the possibility of relatively fresh water in fracture zones below salty units even at depths of a few kilometers. The domination of the topographic driving force implies that deep saltwater is not necessarily stagnant, and significant saltwater flows may be expected to occur in well-connected horizons even at depth. Local topography variation and fracture zone location combine to create a complex flow field in which local topographic driving forces extend to considerable depth in some areas, whereas regional topographic forces predominate in others. Thus, a pattern may be difficult to discern in measurements of the regional saltwater distribution, although it is clear that the coastal region is the major zone of discharge for deeper pre-Holocene fluids. During the land-rise period, regional flow equilibrates with changing climatic conditions and coastal positions, while the distribution of flushing water and older waters lags and will perpetually change between successive glaciations.

CONTENTS ii

Introduction

Little is known about large-scale fluid flow in low-permeability regions of the subsurface. Recent attention has been focussed on such systems, however, due to plans for disposal of toxic wastes at depth. Safety analysis of proposed subsurface storage facilities for nuclear waste entails difficult questions about hydrology. Knowledge of fluid fluxes at repository depths is required in order to calculate degradation rates of engineered barriers. Knowledge is required of how toxic radioactive nuclides, that accidentally leak from a repository, would migrate from the first few tens of meters near the repository to possible distances of tens of kilometers through the bedrock during thousands of years before arriving at the surface or other points of discharge. It may indeed be currently practical to make predictions concerning such migration should it occur in some relatively permeable and homogeneous porous media such as extensive alluvial deposits or other regional aquifers (Bredehoeft and Maini, 1981). However, nuclear waste disposal is targeted for low-conductivity media which are often extremely heterogeneous, and not yet satisfactorily characterized.

In Sweden, nuclear waste facilities are intended for siting below the water table in Sweden's crystalline basement, which while relatively impermeable where intact, is actually highly fractured, with fracture lengths and spacings ranging from meters to tens of kilometers or more. Any safety analysis of a waste repository that considers nuclide migration in such a setting must take into account the complex network of fractures through which primary transport would occur should the repository leak. Also, saltwaters are found at relatively shallow depths in Sweden, and if the flow field is affected by variable fluid density, safety analysis must consider this as well.

While some measurements can possibly be made in the field to characterize small-scale (less than one kilometer) flow and transport through a fractured crystalline fabric, large-scale flow behavior (1 km to 100 km) is not amenable to direct measurement. Rather, in order to gain some understanding at the large-scale, the approach suggested here is to

use a numerical model to simulate regional flow, and analyze the flow behavior under various complicating conditions. The large-scale conditions which the numerical model represents may then be indirectly corroborated through field measurements; alternatively, field evidence may indicate that some aspects of the model are not reasonable, a result which also increases understanding of such systems.

The present investigation has been a part of a Swedish Nuclear Power Inspectorate (SKI) study called, 'SKI Project-90' (SKI, 1991). SKI Project-90 is an integrated performance assessment of a hypothetical high-level nuclear waste repository placed deep in crystalline rock. The purpose herein is to evaluate (via numerical simulation) the major hydrogeologic parameters and features which control regional-scale variable-density fluid flow in the fractured granodioritic rock of Sweden. The analysis illuminates some modes of regional flow-field behavior, and their dependence on the characteristics of the regional fracture network.

The approach taken in the present study is to conduct a generic study of regional flow systems in fractured bedrock in the spirit of Toth (1963, 1980, 1988) and Freeze and Witherspoon (1967). We seek to identify all major controls on regional flow, while not exhaustively studying all possible flow patterns in fractured rocks. Only a few modes of flow behavior are illuminated as these suffice to indicate typical complexities that may exist in large-scale flow through fractured media. The effects of possible value ranges of regional hydraulic parameters as well as of variable fluid density, conductivity dependence on depth, fluid and rock compressibility, surface relief, fracture network pattern, and conductive layers are considered.

Bedrock Hydrogeology and Salt Distribution

Present-day depth-distribution of salt content in fluids residing in Swedish bedrock is not well known on the regional scale, and careful measurements exist at only a few points. It is known, however, that saline waters do exist at depth in many wells and that, in many cases, salt contents are higher than the present-day Baltic Sea. Of wells in Sweden up to 200 m deep that contain saltwater, most occur in locations below the highest post-glacial coastline (FIGURE 1). Saltwater occurs at various depths unrelated to those expected should the system be in static equilibrium with the Baltic Sea. An inference based on the areal distribution of such wells is that the saltwater originates from inundation by late- and post-glacial precursors of the Baltic including the Litorina Sea (FIGURE 2a) (Lindewald 1981, 1985; Enqvist, 1981; Lundqvist, 1965) some of which were more saline than the present Baltic.

However, deeper saline waters in the Baltic Shield below the highest coastline and all saline waters found inland of this line have an origin unrelated to the recent inundation, such as (Smellie and Wikberg, 1991) residual metamorphic fluids or rock-water interaction. Growth of deep permafrost layers during previous glacial periods may give rise to salinity increases in deep waters. Saltwater may derive from ruptured saline fluid inclusions near boreholes or tunnel excavations (Nordstrom, 1985, 1989). Canadian shield brines are similar to some Swedish basement fluids and are thought to be meteoric waters affected by rock-water interaction (Frape and Fritz, 1987). The presence of brines (10%-15% salinity) at depths of several kilometers in Sweden's bedrock have also been reported (Juhlin, 1989). However, the Br/Cl ratio may often be used to distinguish marine waters from formation brines (Frape and Fritz, 1987).

Extensive fracturing of the Baltic Shield in Sweden has occurred at microscopic to regional scales. The maximum horizontal stress in Sweden is generally oriented NW-SE, and the compressive force derives from spreading at the mid-Atlantic ridge (Stephansson, 1989). Much of the large-scale fracturing in Sweden that may be mapped on the surface

may be ascribed to shear structures with en-echelon and possibly imbricate fault systems. The Swedish basement has a complex history of fracturing and opening of subsurface flow paths due to both extensional and compressive stresses (Tirén, 1991). However, the location of active shear as indicated by recent earthquake distribution (as well as patterns of older fracturing) appears to be directly related to differential offset at major transform faults along the mid-Atlantic ridge (Talbot and Slunga, 1989). Thus fracturing of the crystalline basement is a large-scale process that may naturally result in regionally-connected paths for fluid movement.

Fracturing is extensive at all scales, as shown for large scale in FIGURE 3, which is a map of lineaments interpreted as rock blocks in central Sweden. Some features may be traced as far as hundreds of kilometers, although it is pure speculation whether or not fluids are indeed conducted along any given feature. Notably, there is geochemical evidence (related to ore deposition) that fracture zones in some geologic settings conduct fluids over distances of several kilometers (Kerrich and Allison, 1978; Etheridge and others, 1983).

While there clearly can be no equally-detailed map of the vertical distribution of such fractures, we may consider the fact that the areal deformations apparent at the surface are accompanied by deformations occurring in zones more or less parallel to the surface. For depths less than 1 km, there is direct evidence that such sub-horizontal zones in Sweden exist. Stephansson (1989) discusses such zones in reference to stress changes with depth in boreholes. Sub-horizontal zones have been found in Sweden at the Äspö Hard Rock Laboratory (Liedholm, 1990), at the Finnsjön field site and in other similar settings (Andersson and others, 1991). These have alos been in the Canadian shield at depths up to 2 km (Frape and Fritz, 1987). In Sweden, evidence of significant fluid flow in fracture zones at depths of several kilometers has also been reported (Rissler-Åkesson, 1990). The sub-horizontal zones have generally been found to be the major conducting features, but this observation may be due to the difficulty of directly measuring flow in correlated sub-vertical features. To date, no field program to directly correlate the lateral

extent of subhorizontal zones or to determine continuity of fluid migration in such zones has been carried out and only indirect evidence exists. Given the importance to fluid and solute migration if such zones act as regional fluid conduits, the possibility is explored in this study, that given time, fluids can travel both vertically and laterally over significant distances through a series of fractures or a continuous fracture in the crystalline rocks.

Hydraulic conductivity values which may be considered reasonable for flow and transport at the scale of a hundred meters or less for both fracture-free bedrock and for fracture zones have been measured at a number of sites in Sweden. Conductivity values are generally found to be log-normally distributed with a geometric mean typically of 10^{-10} m/s and log-conductivity 25 to 75 percentile range of 10^{-11} to 10^{-7} (Winberg, 1989). Some measurements of hydraulic properties also exist in a few deep boreholes in similar rock in other countries and the lower value ranges confirm the lowest values found in Sweden (Juhlin, 1989) although this may be an artifact of the lowest values measurable. Effective porosities for flow in a conductive fracture zone may range as high as 10^{-3} to 10^{-2} (where conductivity is between 10^{-1} and 10^{0} m/s) (Gustavsson and Andersson, 1991). For the less-conductive portions of the rock, effective porosities may be as low as 10^{-5} (Gale and others, 1987).

In conformance with the expectation that horizontal conductivity decreases with depth in the shield due to closure of fractures by the lithostatic load, early studies in Sweden assigned a power function decrease of conductivity with depth as representative of measurements made in boreholes (SKB, 1983). However, in light of the wide scatter in measured conductivity values and the existence of distinct highly-conductive features at depth, such fits have little practical significance. More recent studies have found that conductivity drops by 10 to 100 times below the upper 100 m to 200 m, and has no statistically-significant depth dependence below. At Fjällveden, Sweden, where there are measurements to a depth of 700 m, there is no significant trend in conductivity below 200 m depth (Winberg, 1989). The upper 200 m (of the 700 m depth measured) has significantly higher conductivity than the lower 500 m at the Finnsjön, Sweden, site

(Andersson and others, 1989), and no other depth-dependence is discernable. No significant decrease of conductivity with depth at all has been found at the Äspö Hard Rock Laboratory, near Oskarshamn, Sweden, to a depth of 1000 m; in fact, there are indications of significant conductivity increases with depth (Liedholm, 1990).

Representation of the Regional System

Land-rise Scenario

The evolution of the freshwater body and the movement of the boundary between recharge water and pre-emergence formation fluids during a 10000-yr period of post-glacial land rise in Sweden is studied. While the process has slowed (FIGURE 2b), land-rise due to post-glacial rebound in Sweden continues today at rates of up to 1 cm/yr (Sjöberg, 1989). Maximum ice thickness in Scandinavia was about 3.5 km and the highest shoreline yet found in Sweden is 281 m above present sea level and is dated to 9250 yr B.P. (Wood, 1989).

Because of the limited database, the land-rise scenario is highly simplified, focussing analysis on large-scale, long-term processes. In the scenario considered, the basement rock is initially (10^4 yr B.P.) saturated with saltwater with the highest salinity thought to have existed in the post-glacial precursor of the Baltic Sea which covered the entire area considered. Clearly, the actual fluid distribution must have been more complex, consisting of glacial meltwaters and varying salinity waters recharged below the series of post-glacial lakes and seas that covered the area. However, for the sake of simplicity in investigating the main features of regional flow, a uniform initial distribution is assumed. As the coast retreats, in this scenario, fresh rain water enters the bedrock in the emerging upland region and flows downward and coastward in the subsurface. Growth of the upland area results from regression of the coastline bounding the Litorina-Baltic Sea.

Were the hydrogeologic origin of the salt distribution in a large area of Sweden known with certainty to be the post-glacial inundations and the present distribution of salinity measured at an appropriate spatial density, then such data could be treated as the rough equivalent of a 10000-year regional-scale tracer test. Model analysis of the data would then provide improved understanding of system structure or even give regional values of flow parameters. However, because of the sparse knowledge of present salinity distribution and some uncertainty concerning its origin, strict calibration of a regional model of subsurface fluid redistribution during land rise is not possible. We must then satisfy ourselves with answers to a less definitive, but equally interesting question concerning modes of system behavior under different assumptions.

Nevertheless, the simulated evolution of subsurface fresh- and saltwater bodies in this study helps to visualize the long-term regional flow field under various conditions. Modes of behavior and important controls are found by examining the simulated flow fields generated by the land-rise process under various hydrogeologic conditions. The system is investigated over this time period for particular simple but structurally differing representations of the fractured rock fabric described later and for various boundary conditions and ranges of parameter values.

Note that an alternative interpretation of the saltwater distribution is that regions containing saline water represent regions of 'old' water (with age more than 10^4 yr) in contrast with water recharged after land emergence (the regions of non-saline water). 'Saltwater' and 'old water' may thus be used interchangeably in most discussions.

A roughly east-west section is modelled with the section center located at an arbitrary point somewhere along the east coast of central Sweden. The length of the section modelled is taken to be 40 km and the depth 2 km. (It was determined that results are not sensitive to either dimension.) The rate of land rise and mean slope of the regional land surface assumed for this section are important as they control the magnitude of the regional topographic driving force. A coastal topographic gradient typical of central

Sweden of 0.005, in conformance with the SKI Project-90 reference site (Lindbom and others, 1989; SKI, 1991), is assumed to apply, giving a section dip of 100 m in 20 km (FIGURE 4). The gravity components (based on gravitational acceleration of 9.81 m^2/s) parallel to the sides of the model section are 9.80988 m^2/s downward perpendicular to the surface, and 0.04905 m^2/s coastward along the dip.

For simplicity, a constant rate of coastal regression is assumed at 100 m per 10^4 yr (FIGURE 2b). Initially in the simulations, at a time of -10^4 yr, the coast is 20 km inland of the present coast and 100 m higher than the present sea level. The coast regresses smoothly and at a time of 0 yr, the coast is at present-day location in the middle of the section, and at time, $+10^4$ yr, the coast would be 20 km further east and 100 m lower than today, at the rightmost corner of the section.

Initial salinity in the entire section and the overlying water body is taken to be that estimated for the Litorina Sea (by Munthe as reported by Magnusson and others, 1957), of 0.015 kg dissolved solids per kg fluid (about half as saline as today's seawater). With time the water body becomes today's Baltic Sea with salinity of 0.005 kg dissolved solids per kg fluid, and this change is modelled as occurring at a constant rate with time.

Numerical Model, Boundary Conditions and Fixed Parameters

The physics of fluid movement and solute transport in the crystalline basement cross-section is described by Darcy's Law and standard mathematical relations for fluid and solute mass balances in porous media. Fluid density varies at a constant rate between 1024.99 kg/m^3 at concentration 0.0357 kg dissolved solids per kg fluid, to 1000 kg/m^3 at a concentration of zero. The governing partial differential equations are solved for the model section using the U.S. Geological Survey computer code, SUTRA (Voss, 1984), which is based on the finite-element method in two spatial dimensions. Voss (1984) gives a complete discussion of governing equations and parameters.

Boundary conditions for the SUTRA simulations are shown in FIGURE 5. No fluid flow is allowed across landward, seaward and bottom sides of the domain. This is equivalent to forcing flow to be vertical along the inland boundary, a probably unrealistic condition which does not strongly affect results because of the elongation of the section. The condition at the seaward boundary is far from the region of interest in the section so that it does not affect results. It is shown later that the location of the bottom boundary condition also does not affect results.

The top boundary of the section is specified as a time-dependent known pressure condition. Below the surface-water body, pressures are determined by the weight of the fluid at its current salinity (which decreases with time as described above). As the coast moves downslope, the water depth at any given point on the surface decreases smoothly causing the specified pressure value at each point to decrease. Eventually, at any point, the water depth reaches zero. Thereafter the pressure is fixed at a value of zero, creating a water table with elevation equal to the top of the model section in the expanding upland area above the coastline (see FIGURE 4). Recharge is assumed to be sufficient to maintain the fixed water-table elevation, and enters the model section at a rate determined by hydraulic gradients and conductivity.

Should recharge to the section occur below the Litorina-Baltic Sea at any time, it would have the current concentration of dissolved solids. Water recharged at the water table is assigned a salt concentration of zero.

The finite-element discretization used is shown in FIGURE 6. While fine discretization is often required for simulation of variable-density problems (Voss and Souza, 1987), a relatively coarse mesh suffices for evaluation of key processes in this case. This is because the evolution of subsurface fresh and saltwater bodies is of interest, while the absolute width of the transition zone between fresh and saltwater regions at any point is not of importance. The parameters governing magnitude of dispersion were fixed at the minimum possible values that give spatially-stable solutions to the transport equation for

the mesh used (longitudinal dispersivity for flow in direction parallel to surface, 200 m, longitudinal dispersivity for flow in direction perpendicular to surface, 10 m, transverse dispersivity, 1 m). The molecular diffusion coefficient in fluid is fixed at $5.x10^{-10}$ m^2/s; note this value must be multiplied by porosity to obtain the porous medium effective value. In the ranges of salinity and temperature considered, fluid viscosity variation is less important to fluid mobility than permeability distribution; thus, fluid viscosity was fixed at 10^{-3} kg/m/s.

Constant time discretization steps of 100 yr are taken, and simulation results are usually examined at $-5x10^3$ yr and 0 yr (every 50 time steps). Results for later times (e.g. at $5x10^3$ yr and 10^4 yr) conform in a predictable manner with early time results; these are not examined herein.

Representations of the Bedrock Fabric

Two simple representations of the fractured heterogeneous shield rock as a porous medium are used in this study. In the **homogeneous models**, the fractured fabric is represented by a porous medium with parameters that are constant or smoothly varying in space. Parameter values are in some sense equivalent to mean or effective values of the heterogeneous fabric. In the **heterogeneous models**, large-scale fracture zones are represented as discrete high-conductivity sections within a matrix of lower effective conductivity material. The latter material represents bedrock with less extensive or more poorly connected fractures. For the heterogeneous models, only a few simple geometries of such fracture zones are considered in order to illustrate some possible modes of regional flow in heterogeneous fabrics. In order to allow comparison, the heterogeneous models are designed to roughly reproduce the regional transmissivity of the homogeneous models.

Effective porosity in a homogeneous model is a complex parameter reflecting the fractional bulk cross-section of flowing channels in any direction, and it generally has a lower value than the total porosity. Its value affects neither the pressure distribution in bedrock nor the fluid flux, but controls actual velocity of groundwater flow. A narrow range of regional effective porosity values considered here in all models suffices to illustrate its effect on transport. The range is between values obtained from laboratory measurements on small samples (10^{-4}) to values typically obtained from field tracer measurements (10^{-3}).

Homogeneous Models

If a fracture network has a 'fine enough' scale of heterogeneity, then regional flow behavior will depend on some mean properties of the network. A homogeneous model will then roughly reproduce the actual regional flow field and salt distribution in such a network. Conductivity values for the homogeneous models are determined by assuming a simple vertical and horizontal fracture-zone distribution making a network of permeable flow paths. The effective directional transmissivity of the network and equivalent mean horizontal and vertical conductivity of the entire section may be calculated as described in the following, where basic parameter values and fracture spacings are drawn from the SKI Project-90 reference site (Lindbom and others, 1989; SKI, 1991). The simple geometry and spacing of the equivalent fracture network considered are shown in FIGURE 7.

Fracture zones are assigned a hydraulic conductivity parallel to the zone of $2.x10^{-7}$ m/s, and the rest of the material, consisting of bedrock blocks with less-connected minor fractures and fracture zone material in the direction perpendicular to the zone, are assigned a value of 10^{-10} m/s. Assuming one 40 m thick horizontal fracture zone per kilometer depth, gives an equivalent horizontal conductivity of the composite medium of about 10^{-8} m/s. Assuming one 50 m wide vertical fracture zone per 5 km lateral distance in both horizontal directions (i.e. both north-south and east-west trending zones), gives an equivalent vertical conductivity of the composite medium of about 10^{-9} m/s. (These

values assume that there is no depth dependence of conductivity in major fracture zones. Depth-dependence is considered separately later.) Thus, for a network of both extensive horizontal and vertical fracture zones, the ratio of horizontal to vertical equivalent conductivity is 10 to 1 (homogeneous model A). Alternatively, if it is assumed that the vertical zones exist but no regionally-connected horizontal zones exist, then the horizontal equivalent conductivity takes on the lower block value, and the horizontal to vertical equivalent conductivity ratio is 1 to 10 (homogeneous model B). The total and effective porosity of a homogeneous model are the same. A value of 10^{-3} is employed (except where noted) as the equivalent of one hundredth of the cross-sectional area participating in flow, where this portion has a flow porosity of 10^{-1}.

Heterogeneous Models

Continuous Horizontal Fracture Zones: This model represents the case where there are extensive horizons or lateral chains of units relatively more permeable than the surrounding matrix. Two cases are considered. The first is homogeneous model A (with $K_H/K_V=10$) with an additional 100 m thick conductive layer having 10 times the horizontal conductivity of the background fabric (10^{-7} m/s). In two variations, the layer is alternatively located at the surface (FIGURE 8a) or at 500 m depth (FIGURE 8b). In the second case, two additional conductive layers (with horizontal conductivity, 10^{-7} m/s) are included, but the horizontal conductivity of the background fabric has a low value typical of blocks (10^{-10} m/s). This case is simply homogeneous model B ($K_H/K_V=0.1$), with additional conductive layers. In this second case, the equivalent horizontal conductivity of the regional system is similar to that of homogeneous model A ($K_H/K_V=10$), whereas in the first case, the equivalent conductivity is somewhat higher. The two layers are alternatively located at the surface and at 500 m depth (FIGURE 8c), or at 500 m and 1500 m depth (FIGURE 8d). The total porosity of these models is 10^{-3} giving an effective porosity for the section of about 10^{-4} for flow in the direction of the layers.

Block-faulted Horizontal Fracture Zones: In this representation, the block-faulted layers have the same properties as the layers described above (in reference to FIGURE 8c), but

are assumed to have been tectonically shifted up and down resulting in horizontal discontinuity at vertical fault zones (FIGURE 9). Vertical conductivity is assumed to be the same everywhere with the same effective vertical conductivity as in the homogeneous models (10^{-9} m/s). Horizontal conductivity in the background matrix is that of the bedrock without connected fracture zones (10^{-10} m/s). Total and effective porosity are the same as for the case of continuous layers, described above.

Intersecting Continuous Fracture Zones: This representation employs a simple block pattern of horizontal and vertical high-conductivity continuous fracture zones (FIGURE 10) similar to the network depicted in FIGURE 7. The fracture zones have conductivity parallel to the zone of 10^{-7} m/s. Block conductivity and conductivity perpendicular to zones is 10^{-10} m/s. A number of cases are considered where block conductivity ranges up to 10^{-8} m/s. Total porosity is again 10^{-3} (except where noted) resulting in an effective porosity of about 10^{-4} for both horizontal and vertical flow. For the case with higher block conductivity, effective porosity ranges to nearly 10^{-3} because significant flow occurs in most of the cross-section.

Results of Simulations

A large number of simulations based on different models of the bedrock fabric or parameter values were examined. Only the most distinguishing results are presented and evaluated in the following.

General - Homogeneous and Heterogeneous Fabrics

Regional Flow Field: Regional flow is generally driven by the mean gradient of the water table which follows land surface topography. This is shown in FIGURE 11 for homogeneous model A with $K_H/K_V = 10$. Note that in all figures, the Litorina-Baltic Sea water level and coastline are indicated; the location of water recharged after emergence

is indicated by contours following isopleths of volumetric percent of residual old fluid; and fluid velocity vectors are given, depicting the flow field. Vector lengths are proportional to velocity, and the reference velocity given in the figure caption is for a vector length of one-tenth of the vertical side of the section. All vector directions are corrected to account for the vertical exaggeration of 10. Where indicated in later figures, vector lengths are proportional to the logarithm of velocity magnitude.

Freshwater flows downward from exposed upland areas creating an ever-growing freshwater body that replaces saltwater in the bedrock. Both fresh recharge water and displaced saltwater flow towards the coast and discharge primarily at the coastline. The discharge point follows the coastline as the coast regresses. Very little regional flow passes seaward of the coast because of the low hydraulic gradient under the simulated Baltic Sea compared with the topographic gradient, a result in agreement with the work of Bredehoeft and Maini (1981). Minor topographically-driven flow would occur below the Baltic under some conditions, because as the Baltic water freshens, a hydraulic gradient develops in the saltier bedrock fluid. Baltic water is driven down into the bedrock near the coast, and subsurface fluids flow towards a discharge area near the deepest simulated portion of the sea. However, the rate and time-dependence of concentration change in the Baltic has negligible impact on the flow field (tested by simulation, but not shown) in all situations examined. For homogeneous model A, the growth of the subsurface body of fresh recharge water lags a few kilometers after the coastal position (FIGURE 11). In homogeneous model B, with effective transmissivity 100 times less than model A, lateral flow is 100 times slower and freshwater hardly moves past the inland boundary in 10^4 yr (FIGURE 12).

Regional Recharge: Recharge in the model is controlled both by conductivity and by the vertical gradients in hydraulic head along the exposed water table above the coastline. The total regional flux of freshwater does not vary greatly among the various situations tested. The range is from 6×10^{-5} kg/s (5×10^{-3} m^3/day) to 12×10^{-5} kg/s (1×10^{-2} m^3/day) per meter cross-section thickness. Associated Darcy fluxes for flow occurring over the entire section depth range from 9×10^{-4} m/yr to 2×10^{-3} m/yr. This range includes all of the

situations with differing exposed surfaces, differing parameter values, and various fracture networks that are discussed later. This reflects the intended similarity in net transmissive properties of the various bedrock fabric representations. The exception is homogeneous model B with recharge of only $1x10^{-6}$ kg/s ($9x10^{-5}$ m^3/day), because of the significantly lower lateral transmissivity of this model.

Effect of Bottom Location: Only horizontal flow is allowed at the bottom boundary of the section analyzed. The depth chosen for this boundary is arbitrary, and, in the range from 2 km to 4 km, its position has little effect on the flow field (compare FIGURE 11b and FIGURE 13). If conductivity decreases with depth, the position of the bottom boundary would become even less important.

Effect of Compressibility: Compressibility of the system, if bedrock compressibility is similar to or less than that of water, causes only minor lag in the motion of the transition zone as it follows the coast (simulated but not shown). Thus, assumption of a quasi-steady pressure field (or zero compressibility) is possible for regional analysis.

Effect of Variable Fluid Density: In variable-density fluids, there often occurs some circulation in the flow field. Should such circulation be strong in the section modelled, there would be a small component of flow directed inland below some depth in the bedrock. In both homogeneous and heterogeneous fabric types and under all circumstances considered, however, this component is overwhelmed by the topographically-driven flow occurring as a result of the water table following the mean inclination of the land surface. Thus, even at depth in saline waters, regional-scale flow is directed downslope or coastward. Moreover, simulations conducted without differences in fluid density exhibit only minor increases (approximately 50% greater) in fluid velocities at depth, and a somewhat deeper freshwater body (compare FIGURE 14 and FIGURE 11b). Because variable fluid density only has a small effect on the flow field during land rise, the hydraulic boundary conditions and the ratio of hydraulic conductivity to porosity are the main controls on the local fluid velocity.

Regional Porosity: Porosity controls the total fluid volume of the fabric in the simulation. Given a fixed recharge rate, freshwater sweeps out old saltwater in the section ten times faster when the porosity is ten times lower. FIGURE 15 shows that, for homogeneous model A with a porosity reduced to 10^{-4}, the freshwater-saltwater distribution does not lag behind coastal movement to a depth of at least 2 km. This, however, is an unrealistic result for the Baltic Shield as it does not agree with observed salinity patterns. Thus, the ratio of horizontal conductivity to porosity must be significantly less than 10^{-4} m/s (the value in this case) in a homogeneous system for results to be representative of the situation in Sweden. For homogeneous model B with porosity 10^{-3} (and reduced recharge because of its lower transmissivity), the ratio is 10^{-7} m/s, resulting in unrealistically slow flushing of old waters (FIGURE 12). Thus, a reasonable range for the ratio in a homogeneous model representation of the Swedish basement may be from about 10^{-6} m/s to 10^{-5} m/s. The latter value is that of homogeneous model A.

Transient Conditions: Under land-rise conditions, simulations show that the flow field is in a transient state as long as the coast does not remain stationary for a long time (i.e. on the order of 10^5 years). Equilibrium conditions and slow landward circulation of saltwater would occur only after the transient flushing process driven by land rise ends. In the simulation shown for homogeneous model A (FIGURE 16), the coast location and the salt concentration in the Baltic are held constant from the present time (0 yr) into the future. While some density-driven circulation begins at about $3x10^4$ yr, equilibrium conditions are not achieved even after 10^5 yr because old saltwater still remains to be flushed out below the Baltic.

Effect of Heterogeneous Fabrics

Continuous Horizontal Fracture Zones: Extensive layers or lateral chains of units relatively more permeable than the surrounding matrix are the primary conductors of fluid on the regional scale. Migration of the freshwater front due to coastal regression in the simulations is significantly advanced in such layers relative the bedrock matrix, such that freshwater may sometimes be found in such layers below zones of saline water (compare

FIGURE 17 and FIGURE 18 with FIGURE 11b). In the land-rise scenario, freshwater always discharges near the regressing coast, and depending on system parameters, a layer as deep as 500 m can flush out the saline water in shallower low conductivity layers. Alternatively, depending on relative motions of the coast, fluid flow in a series of layers can leave behind regions of saline water in low conductivity regions (FIGURE 19 and FIGURE 20).

Block-faulted Horizontal Fracture Zones: High fluid flux in a layer is distributed through the matrix when fluid reaches a fault boundary, and seeks the least hydraulically-resistive path to the high conductivity zone which is down-gradient. The evolution of the salinity distribution during land rise in this model is complex (FIGURE 21). Freshwater 'channels' are formed that connect the high-conductivity layers through the low-conductivity matrix. Islands of saline or old water are left behind the spatially-complex freshwater front. Flow in the segmented layers is horizontal, and flow in the matrix is mainly vertical (because the effective vertical conductivity of this model includes the homogeneous analog of vertical fractures, whereas effective horizontal conductivity is based on a fracture-free fabric).

Intersecting Continuous Fracture Zones: Freshwater flows downward, coastward, and then upward towards the discharge, as the proximity of a vertical fracture zone to the regressing coast permits (FIGURE 22). Freshwater can be found in permeable zones at any depth. Saline water can remain in the large blocks of low-conductivity bedrock for 10^5 yr. Saline water is flushed out at a rate determined by diffusion for low block conductivities, and by the conductivity-porosity ratio at higher block conductivity values (compare FIGURE 22b, FIGURE 23, and FIGURE 24). The latter also directly determines the fluid velocity in the block. The flow direction in the blocks depends on the regional flow field in the fracture network and on the block's location in the region. Flow within a block can be in any direction and can change throughout a block. The magnitude of velocity (not Darcy flux) in the fracture zones for all cases is about 4×10^{-7} m/s. The magnitude of velocity in the blocks varies from 4×10^{-10} m/s to 4×10^{-8} m/s as block

conductivity changes from 10^{-10} m/s to 10^{-8} m/s. The general direction of velocity in blocks tends more toward horizontal for higher block conductivity.

Effect of Surface Features

Surface Relief: The roughness or local relief relative to the mean trend of the regional land surface exerts an important influence on the flow field. As the water table usually has the shape of a subdued representation of land surface, local relief causes disturbances in the form of closed flow cells to be superimposed on the deeper regional-scale behavior (as discussed by Toth (1963, 1980, 1988) and Freeze and Witherspoon (1967)). The cell depth is roughly 10 times the amplitude of the water table relief under the conditions and parameter values used in homogeneous model A (FIGURE 25 and FIGURE 26). In these simulations, peak to peak distance between water table ridges is 4 km and two surface amplitudes (valley bottom to top of ridge) 25 m and 50 m, are represented. The elevation relief of the upper model boundary centers on the original surface. In heterogeneous models of the bedrock fabric with surface relief, the only generalization that may be drawn is that cell depth and distribution are highly sensitive to the particular character of the fracture network; cells may be irregularly shaped and either extremely shallow or reaching several kilometers depth (simulated but not shown). In reality, the situation for the Baltic Shield is even more complex; surface relief may have a number of dominant spatial frequencies and amplitudes, and surface elevations may be correlated with the fracture network pattern.

Ridge above Bedrock Block: A simple examination of the effect of surface relief focusses on the disturbance to the regional flow field caused by a single long 50 m ridge. The upper model boundary location at ridge top was raised 50 m above the original surface. In a homogeneous model, a simple local circulation cell develops under the ridge. The cell begins as the ridge top emerges from the receding Baltic, and a freshwater lens develops under the island (FIGURE 27a). Lens discharge occurs at the island shores. Following attachment of the island to the mainland area, regional fluid discharge in the upwards direction competes with downward freshwater flow below the ridge (FIGURE

27b). This may create a stagnation point in the flow field somewhere along the lower surface of the ridge's circulation cell. The depth which the cell reaches in a homogeneous model varies smoothly with the balance of topographic driving forces and hydraulic parameters.

In the heterogeneous fabric with intersecting continuous fracture zones, when the ridge exists directly over a bedrock block, the flow field exhibits two distinct modes of behavior (compare FIGURE 28 and FIGURE 29). An examination of the flow field for $t=-5x10^3$ yr with a range of block conductivity shows that for regional block conductivity greater than about 1/600 of regional fracture conductivity (more than $1.8x10^{-10}$ m/s), flow in the blocks directly below the ridge is downward (as in FIGURE 28a). When regional block conductivity is less than about 1/600 of regional fracture conductivity (less than $1.4x10^{-10}$ m/s), flow in the blocks directly below the ridge is upward (as in FIGURE 29a). As the conductivity varies smoothly among simulations, the location of the stagnation point changes suddenly from the bottom of the cross-section to the uppermost conductive zone at a value near $1.6x10^{-10}$ m/s. Thus, in a heterogeneous fabric, cell depth and shape may be extremely sensitive to small differences in network structure or parameter values. In the case of a conic hill in a three-dimensional flow field, the sensitivity of the stagnation point's depth may be quantitatively different, but the general behavior to be expected is the same.

Importance of Conductivity Dependence on Depth

The depth distribution of effective conductivity is an important control on the regional flow field, even if the conductivity decrease is mild (i.e. proportional to depth). Flux through the region is concentrated near the surface when conductivity decreases with depth resulting in significantly greater near-surface velocities than in cases without depth dependence. Results are shown here for the homogeneous model with 50 m surface relief, wherein conductivity is assumed constant for the upper 100 m. Below 100 m, conductivity decreases in inverse proportion to additional depth (FIGURE 30), or even

more slowly, in inverse proportion to one tenth of additional depth (FIGURE 31); compare with FIGURE 26.

Near-surface concentration of regional flux also occurs in heterogeneous models when major fracture zones undergo even a mild depth-dependent decrease. Results are shown in FIGURE 32 (compare with FIGURE 22b) for a simulation where conductivity in the heterogeneous model with intersecting continuous fracture zones is decreased with depth as follows: no change in original conductivity of the uppermost 100.m, then, a smooth drop of fracture zone conductivity to one tenth of its original value by 1 km depth, and to one hundredth of its original value by 2 km depth. The deepest horizontal fracture zone is 10 times more conductive than the bedrock blocks. The resulting flow field is insensitive to block conductivity which is held constant at 10^{-10} m/s. However, even when fracture-zone conductivities decrease with depth, velocities within such zones can still be significant. FIGURE 33 shows freshwater moving through deep layers in the same fabric in a system where porosity is ten times lower (10^{-4}) than in the former model (FIGURE 32).

Discussion of Results

Inspection of the simulations presented shows that the most important parameters controlling fluid velocity and distribution of salinity for a homogeneous model of Baltic Shield rock are horizontal and vertical conductivity, and effective porosity. As expected, system transmissivity controls net fluid flux through the system, while the ratio of hydraulic conductivity to effective porosity controls actual fluid velocity. For a heterogeneous model consisting of a network of high-conductivity paths in a low-conductivity matrix, the most important additional parameters are the conductivity contrast between the network of paths and the matrix, as well as the connectivity and geometry of the network. Very small changes in regional hydraulic parameters can have strong effects both on the direction and magnitude of local velocities in heterogeneous fabrics. Although forces due to

variable-density exist in the system, they are, for the density differences considered, much less than topographic forces, allowing the water-table topography to be the primary driving force for flow at all spatial scales.

Flow in relatively impermeable bedrock blocks within a network of conductive fractures may be in any direction. The direction may change throughout a block. Further, the general flow direction in a block cannot simply be predicted on the basis of a knowledge of local topography, fracture zone locations, and local hydraulic parameters.

The magnitude of mean velocity of flow through a bedrock block depends on the block conductivity, effective porosity, and on the hydraulic gradient across the block. The mean Darcy flux through a block depends on conductivity and gradient, but not on porosity. The range of possible hydraulic gradient across a block is limited to a maximum value obtained by considering the maximum water-table relief in the geographic region and applying this difference directly across the block. This is the special case where the fracture network conducts relatively undiminished fluid pressure levels from distant locations directly to the block. Thus given a range of possible conductivities (and porosities) the maximum possible mean velocity (and mean flux) magnitudes through a block may be predicted. Of course, the actual conductive network within each block probably behaves as a scaled-down version of the regional network, making detailed prediction of the spatial distribution of velocity magnitudes and direction virtually impossible from field measurements.

The surface relief, fracture zone geometry, and regional parameter values have a complex interaction in producing a flow field in the Baltic Shield. The flow field in a given closed cell near the surface would also be virtually impossible to predict on the basis of field measurements. Small differences in fracture connectivity or fracture or block conductivity can give rise to completely different flow fields although pressure values may not display measurable sensitivity to these factors.

Conductivity-dependence on depth of conductive fracture zones is an important parameter controlling the lateral regional flux of fluids at depth. However, if fracture zones exist at depth, as long as they are more conductive than their surroundings, then the characteristics of the network they make up are a major control on the regional flow field.

The existence of variable-density fluids in the shield (at least for concentrations below standard sea water) has little effect on the transient flow field resulting from land rise and coastal regression. The fact that salty water exists at depth in Sweden's bedrock is, by itself, not sufficient evidence that the flow field is stagnant. On the contrary, both fracture zone and intra-block velocities in saltwater at any depth may be expected to be of the same magnitude as in freshwater because flow is driven mainly by topographic gradients and land-rise. Should the flow in the saltwater, in a localized region, actually be significantly slower than in the freshwater, it is due only to the fact that the rocks in which saltwater locally occurs happen to have low transmissivity.

The present-day salt distribution in the Baltic Shield in Sweden is likely spatially complex with saltwater (of arbitrary geologic origin) residing both in blocks with low transmissivity and in regionally-connected fracture zones. There is a likelihood that relatively freshwater exists in conductive zones below regions of saltwater.

Most freshwater and saltwater flux through the shield will eventually discharge near the coast, in other major regional discharge areas, or in the case of fluids that circulate in local cells, at local discharge areas. In other words, the deep saltwater is not an isolated or stagnant flow system, and deep fluids will eventually discharge at the surface near the coast or below the sea. This phenomenon has been studied by Toth (e.g. Toth, 1980), where salt marshes are explained as resulting from discharge of deep fluids. Possible evidence of deep fluid discharge in the form of salt springs have been found in a number of locations, such as Ontario, Canada (Frape and others, 1984), and the Skara plain south of Lake Vänern in Sweden (Lindewald, 1985).

The regional groundwater system of the Baltic Shield in Sweden is in a perpetual non-equilibrium state following hydrologic and climatic stresses. The pressure distribution likely remains in quasi-equilibrium with boundary conditions and with the fluid density distribution because of low system compressibility. However, the density distribution and the dissolved salt distribution likely lags 10^4, 10^5, or more years after coastal movement. Because flow is relatively independent of salt concentration, the flow field may remain in relative equilibrium with the coastal position at any time. However, the regional salt distribution likely never attains equilibrium with hydraulic stresses induced by succeeding glaciations which have periods on the same order as the lag time. While the flow field may equilibrate with changing topographic driving forces, the 'turn-over time' of resident fluids is such that significant quantities of old fluids always exist in low conductivity blocks and/or at depth. Indeed, it is possible that the age-distribution of subsurface fluids reflects an accumulation of flushing and saltwaters from previous glacial-climatic cycles.

Conclusions

In much of the Baltic Shield, there exists salty water at depth ranging in salinity from values typical of present sea water in the shallower depths of a few hundred meters, to brines at depths of a few kilometers. The deeper brines result from chemical rock-water interactions, whereas the upper saltwaters, particularly in the regions below the highest post-glacial coastline, may be marine. For depths of a few hundred meters, waters are likely to be of post-glacial sea origin. If 10000-year-old saltwater indeed exists at shallow depths, then this may be taken either as an indication of slow fluid movements through the bedrock over long times, or of large travel distances through fracture systems before arriving at measurement points. Questions arise, about the importance of the variable density in the fluids to the behavior of the flow field. Strong density effects would imply a circulating saltwater system that occurs below the freshwater, with saltwater velocities directed inland below some depth. Further questions arise about the changes in the flow

field in the future after the existing inland saltwater is swept out of the bedrock. This analysis has considered the long-term regional behavior of variable-density fluid flow through the Baltic Shield in Sweden during the period of Holocene flushing.

Simulation of a 40 km long cross-section of Sweden's basement rock extending 20 km into the present-day Baltic Sea with post-glacial land-rise and coastal regression has the following major results. During the period of land-rise, the variable density of fluids in the upper few kilometers of the bedrock has little effect on the regional flow behavior. Rather, regional flow is driven primarily by the topography of the water table, as it changes during post-glacial land rise. Coastal regions (or large deep lakes) are the major zone of discharge for deeper fluids. If land rise were to stop and the coast become stationary, it would take tens of thousands of years to establish steady circulation conditions driven by the variable-density of ambient fluids. Thus, in practical terms, variable-density effects may be disregarded in analyses of the regional flow fields during land rise in favor of topographic driving forces. Further, it is found that the existence of 'old' saltwater in portions of the bedrock is <u>not</u> indicative of variable-density effects causing a slow or stagnant flow field in the saltwater. The existence of saltwater at any point is either due to the fact that the conductivity or connectivity of local conductive structures in the bedrock is poor, or that older waters have travelled to the measuring point from some distance away through conductive fracture systems. In summary, the presence of saltwater is consistent with the notion of incomplete, but ongoing, Holocene flushing of the basement.

The simulations also illustrate that the actual distribution of saltwaters in bedrock is highly dependent on both regional and local geometry and connectivity of conductive structures in the bedrock, as well as on the surface topography. Distribution of freshwater and saltwater in the Baltic Shield in Sweden may be expected to be discontinuous, with the possibility of relatively freshwater in fracture zones below salty units even at depths of a few kilometers. A regional pattern of saltwater distribution may be difficult to discern by field measurements as local topography variation and fracture zone location may combine

to create an exceptionally complex picture, in which local driving forces may extend to considerable depth in some areas whereas regional forces may predominate in others.

Because the major driving force in the system is the topographic gradient, the saltwater is likely not stagnant, and significant saltwater flows may be expected to occur in well-connected fracture zones even at considerable depths. During the land-rise period, the regional flow field remains in a quasi-steady state with climatic conditions and coastal positions as they change with time. However, simulations show that the saltwater distribution lags considerably, and is perpetually in a non-equilibrium state between successive glaciations.

These results have direct implications for safety analysis of high-level nuclear waste facilities sited in crystalline rock. The safety of such a nuclear waste repository in part relies on the bedrock as an effective barrier to escaping radionuclides, reducing possible doses reaching the biosphere over periods of thousands to tens of thousands of years or more following waste emplacement. A safety analysis may disregard variable-density as a driving force for regional flow and fluids may be considered to have approximately uniform density. However, coastal regression must be included in analysis that predicts the regional flow field during long times. Over such time periods in fractured rock, radionuclides may travel many kilometers in any direction with flowing groundwater before reaching the surface near the coast (or other regional or local discharge area) if they are not hindered by other processes which restrict mobility chemically. Thus, safety analysis must include regional driving forces for fluid and radionuclide transport.

Field measurements of hydrogeologic parameters controlling groundwater flow including geometry and connectivity of inferred fracture networks, are by their nature limited to scales over which artificial stresses can be induced, usually 1 km or less. One might suggest that field studies consisting of hydraulic and tracer tests on a grid pattern of 1 km squares (should such be economically possible), when considered en masse would

give the required information on the regional scale. Careful consideration and the present study, however, indicate that this is not necessarily true in the crystalline basement without complete knowledge of how each local area fits into the regional structure. Only a field test stressing a region at the scale of interest (and of sufficient depth) would give certain information about the flow regime at that scale. Possibly, corroboration of existing geochemical distributions in subsurface fluids with hydrogeologic data would give more insight into regional flow than either approach alone.

There is great practical difficulty (maybe impossibility) of obtaining such large-scale information through direct measurement. Thus, another approach to the large scale is required if the fate of possible leaks from a nuclear waste repository is to be evaluated. Because the approach to answering this question, whatever it is, cannot ever be tested at the scale of application, we must rely on indirect means of building confidence in our ability to cleverly interpret available facts and make judgements about large-scale transport. Some confidence is gained by developing, as attempted in this study, an appreciation of the controls that may affect regional-scale flow in fractured crystalline fabrics.

References

Andersson, J.-E., Nordqvist, R., Nyberg, G., Smellie, J., and Tirén, S., Hydrogeological conditions in the Finnsjön area - Compilation of data and conceptual model, Arbetsrapport 89-24 Forskning och Utveckling, SKB (Swedish Nuclear Fuel and Waste Management Co.), Stockholm, Sweden, 1989.

Andersson, J.-E., Ekman, L., Nordqvist, R. and Winberg, A., Hydraulic testing and modelling of a low-angle fracture zone at Finnsjön, Sweden, J. Hydrol., 126(1-2), 45-77, 1991.

Bredehoeft, J.D. and Maini, T., Strategy for radioactive waste disposal in crystalline rocks, Science, 213(4505), 293-296, 1981.

Enqvist, P., Some wells with high content of chloride in central Sweden, in "Intruded and Relict Groundwater of Marine Origin - Proceedings of the Seventh Saltwater Intrusion Meeting," Geological Survey of Sweden Report Number 27, 33-39, Uppsala, Sweden, 1981.

Etheridge, M.A., Wall, V.J. and Vernon, R.H., The role of the fluid phase during regional metamorphism and deformation, J. Metamorphic Geol., 1(3), 205-226, 1983.

Frape, S.K. and Fritz, P., Geochemical trends for groundwaters from the Canadian shield, in "Saline Water and Gases in Crystalline Rocks," edited by Fritz, P. and Frape, S.K., Geological Association of Canada Special Paper 33, 19-38, 1987.

Frape, S.K., Fritz, P. and Blackmer, A.J., Saline groundwater discharges from crystalline rocks near Thunder Bay, Ontario, Canada, in "Hydrochemical Balances of Freshwater Systems," edited by Eriksson, E., IAHS-AISH Publication No. 150, 369-379, 1984.

Freeze, R.A. and Witherspoon, P.A., Theoretical analysis of regional groundwater flow; 2. Effect of water table configuration and subsurface permeability variation, Water Res. Res., 3(2), 623-634, 1967.

Gale, J., Macleod, R., Welhan, J., Cole, C., and Vail, L., Hydrogeological characterization of the Stripa site, Stripa Project Technical Report 87-15, SKB (Swedish Nuclear Fuel and Waste Management Co.), Stockholm, Sweden, 1987.

Gustavsson, E. and Andersson, P., Groundwater flow conditions in a low-angle fracture zone at Finnsjön, Sweden, J. Hydrol., 126(1-2), 79-111, 1991.

Juhlin, C., Storage of nuclear waste in very deep boreholes: Feasibility study and assessment of economic potential, Part I - Geological considerations, Technical Report 89-39, 102 pp., SKB (Swedish Nuclear Fuel and Waste Management Co.), Stockholm, Sweden, 1989.

Kerrich, R. and Allison, I., Vein geometry and hydrostatics during Yellowknife mineralisation, Can. J. Earth Sci., 15(10), 1653-1660, 1978.

Liedholm, M., Some notations on the correlation between the hydraulic conductivity and the vertical depth based on information from KAS02-KAS08 - Technical note 14, in "Conceptual Modelling of Äspö, Technical Notes 1-17, General Geological, Hydrogeological and Hydrochemical Information,", edited by Liedholm, M., Äspö Hard Rock Laboratory Progress Report 25-90-16a, SKB (Swedish Nuclear Fuel and Waste Management Co.), Stockholm, Sweden, 1991.

Lindbom, B., Lundblad, K., and Markström, A., Initial groundwater flow calculations at the SKI reference site, SKI-TR 89:2, Swedish Nuclear Power Inspectorate, Stockholm, Sweden, 1989.

Lindewald, H., Saline groundwater in Sweden, in "Intruded and Relict Groundwater of Marine Origin - Proceedings of the Seventh Saltwater Intrusion Meeting," Geological Survey of Sweden Report Number 27, 24-32, Uppsala, Sweden, 1981.

Lindewald, H., "Salt grundvatten i Sverige" (Saline groundwater in Sweden), Geological Survey of Sweden Report Number 39, Uppsala, Sweden, 1985.

Lundqvist, J., The Quaternary of Sweden, in "The Quaternary - Volume 1," edited by Rankama, K., pp. 139-198, Interscience Publishers, New York, 1965.

Magnusson, N.H., Lundqvist, G. and Granlund, E., "Sveriges geologi," (Sweden's Geology), Scandinavian University Books - Norstedts, Stockholm, Sweden, 1957.

Nordstrom, D.K., Andrews, J.N., Carllson, L., Fontes J.-C., Fritz, P., Moser, H., and Olsson, T., "Hydrological and Hydrogeochemical Investigations in Boreholes -Final Report of the Phase I Geochemical Investigations of the Stripa Groundwaters," Stripa Project Technical Report 85-06, SKB (Swedish Nuclear Fuel and Waste Management Co.), Stockholm, Sweden, 1985.

Nordstrom, D.K., Lindblom, S., Donahoe, R.J., and Barton, C.C., Fluid inclusions in the Stripa granite and their possible influence on the groundwater chemistry, Geoch. et Cosmoch. Acta, 53, 1741-1755, 1989.

Rissler-Åkesson, G., Wireline logging in the crystalline environment of the Gravberg-1 well, RD&D Report U(G)1990/52, Vattenfall (The Swedish State Power Board), Vällingby, Sweden, 1990.

Stephansson, O., Stress measurements and modelling of crustal rock mechanics in Fennoscandia, in "Earthquakes at North-Atlantic Passive Margins: Neotectonics and Postglacial Rebound," edited by Gregersen, S. and Basham, P.W., 213-229, Kluwer Academic, 1989.

Sjöberg, L.E., The secular change of gravity and the geoid in Fennoscandia, in "Earthquakes at North-Atlantic Passive Margins: Neotectonics and Postglacial Rebound," edited by Gregersen, S. and Basham, P.W., 125-139, Kluwer Academic, 1989.

SKB (Swedish Nuclear Fuel and Waste Management Co.), "Final Storage of Spent Nuclear Fuel - KBS-3 - Volume II-Geology," SKB, Stockholm, Sweden, 1983.

SKI (Swedish Nuclear Power Inspectorate),"SKI Project 90", SKI TR-91:23, vol I and vol II, SKI, Stockholm, Sweden, 1991.

Smellie, J.A.T. and Wikberg, P., Hydrochemical investigations at Finnsjön, Sweden, J. Hydrol., 126(1-2), 129-158, 1991.

Talbot, C.J. and Slunga, R, Patterns of active shear in Fennoscandia, in "Earthquakes at North-Atlantic Passive Margins: Neotectonics and Postglacial Rebound," edited by Gregersen, S. and Basham, P.W., 441-466, Kluwer Academic, 1989.

Tirén, S.A., Geological setting and deformation history of a low-angle fracture zone at Finnsjön, Sweden, J. Hydrol., 126(1-2), 17-43, 1991.

Tirén, S.A. and Beckholmen, M., Influence of regional shear zones on the lithological pattern in central Sweden, Geologiska Föreningens i Stockholm Förhandlingar (Geological Society of Stockholm Proceedings), GFF-112, 197-199, 1990.

Tirén, S.A. and Beckholmen, M., Rock block map analysis of southern Sweden, Geologiska Föreningens i Stockholm Förhandlingar (Geological Society of Stockholm Proceedings), GFF-113, 253-269, 1992.

Toth, J., A theoretical analysis of groundwater flow in small drainage basins, J. Geophys. Res., 68(B6), 4795-4812, 1963.

Toth, J., Cross-formational gravity flow of groundwater: A mechanism of the transport and accumulation of petroleum (The generalized hydraulic theory of petroleum migration), in "Problems of Petroleum Migration," edited by Roberts, W.H. and Cordell, R.J., pp. 121-167, American Association of Petroleum Geologists Studies in Geology, no. 10, 1980.

Toth, J., Groundwater and hydrocarbon migration, in "Hydrogeology-The Geology of North America," edited by W. Back, J.S. Rosenshein and P.R. Seaber, vol O-2, pp. 485-502, Geological Society of America, Boulder, Colorado, 1988.

Voss, C.I., SUTRA - A finite-element simulation model for saturated-unsaturated, fluid-density-dependent ground-water flow with energy transport or chemically-reactive single-species solute transport, U.S. Geological Survey Water-Resources Investigations Report 84-4369, U.S. Geological Survey, Reston, Virginia, 1984.

Voss, C.I. and Souza, W.R., Variable density flow and solute transport simulation of regional aquifers containing a narrow freshwater-saltwater transition zone, Wat. Res. Res., 23(10), 1851-1866, 1987.

Winberg, A., Project-90: Analysis of the spatial variability of hydraulic conductivity data in the SKB database GEOTAB, SKI-TR 89:12, Swedish Nuclear Power Inspectorate, Stockholm, Sweden, 1989.

Wood R.M., Extraordinary deglaciation reverse faulting in northern Fennoscandia, in "Earthquakes at North-Atlantic Passive Margins: Neotectonics and Postglacial Rebound," edited by Gregersen, S. and Basham, P.W., 141-173, Kluwer Academic, 1989.

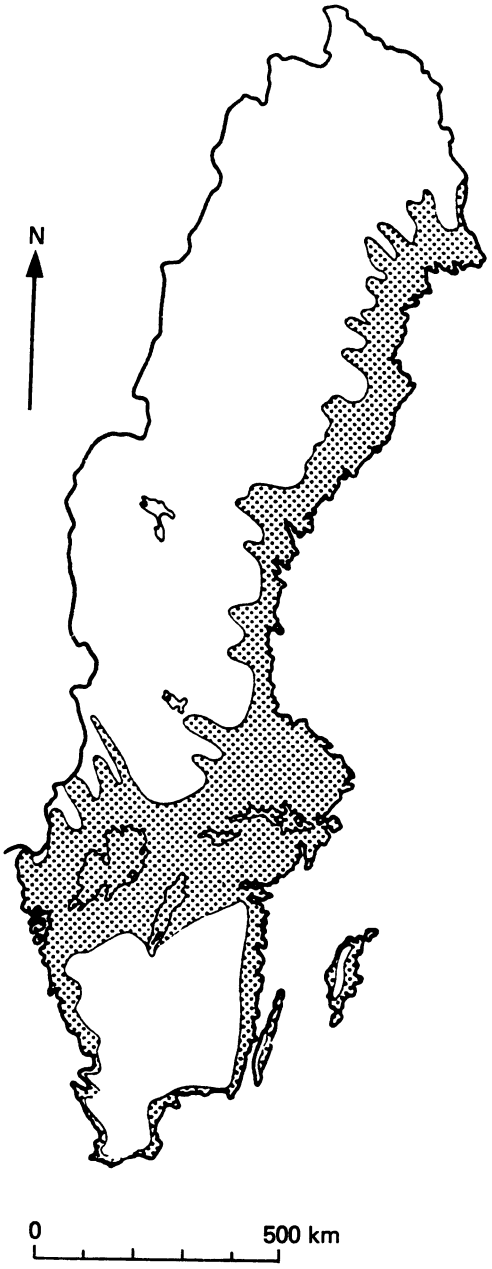

Figure 1 - Holocene marine limit in Sweden, about 10000 yr B.P. (after Lindewald, 1985).

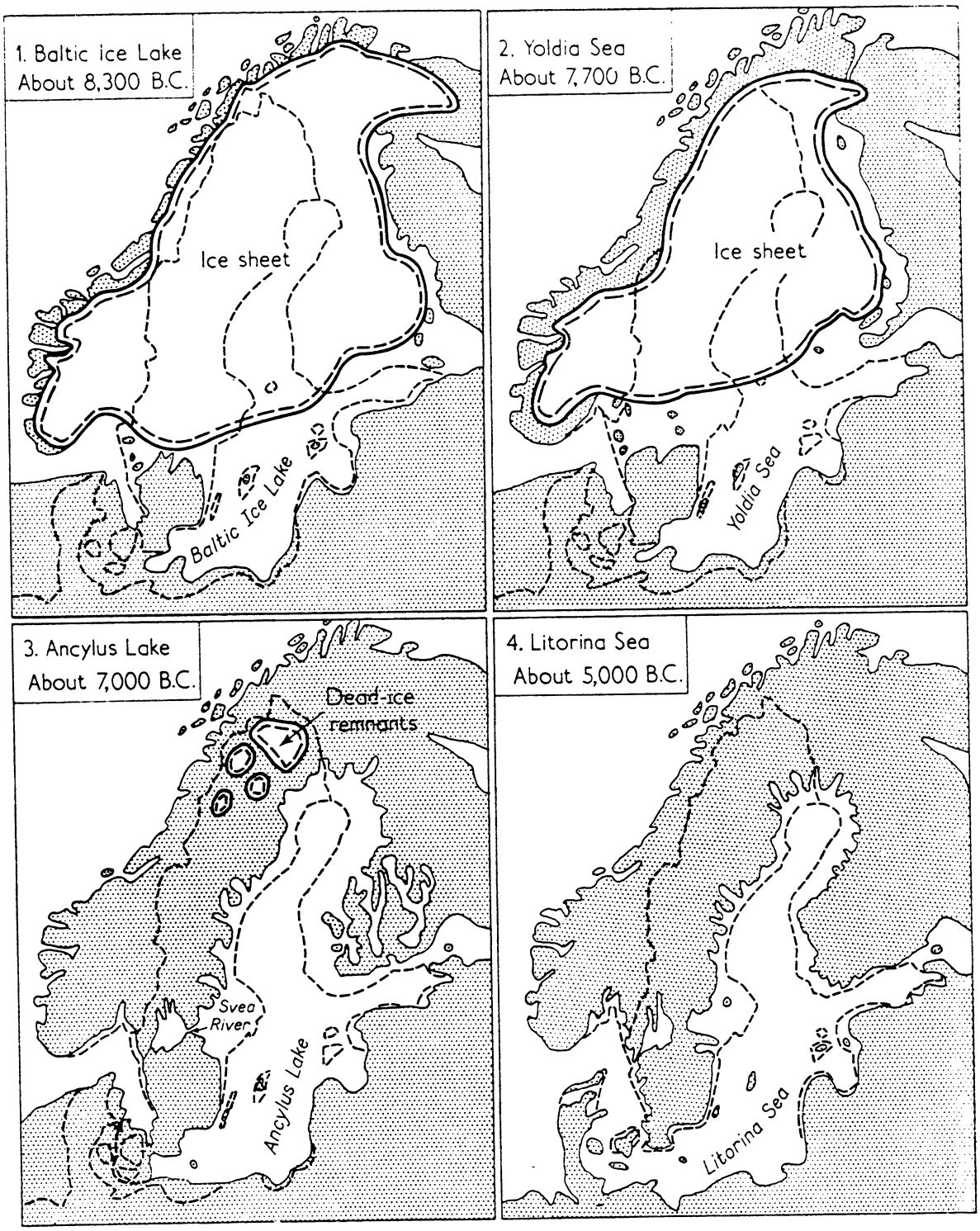

Figure 2a - Holocene precursors of the Baltic Sea (after Lundqvist, 1965).

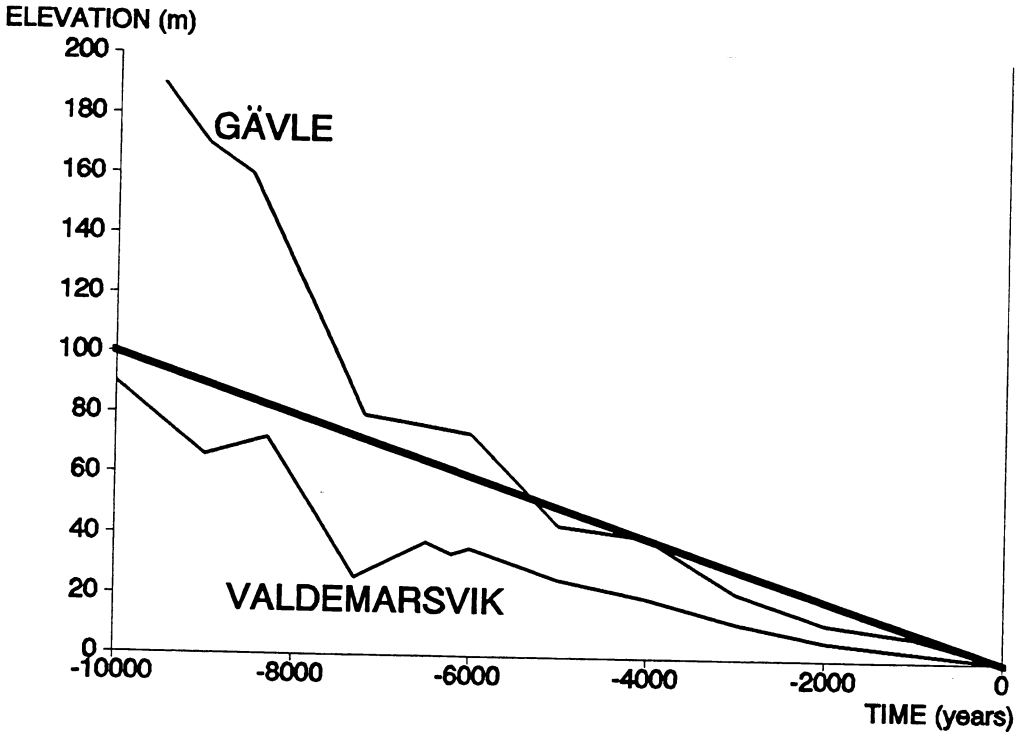

Figure 2b - Coastal regression since 10000 years B.P. at two locations in Sweden showing coastal elevation over present sea level (after E. Granlund as reported by Magnusson and others, 1957). Straight line shows simulated coastal regression.

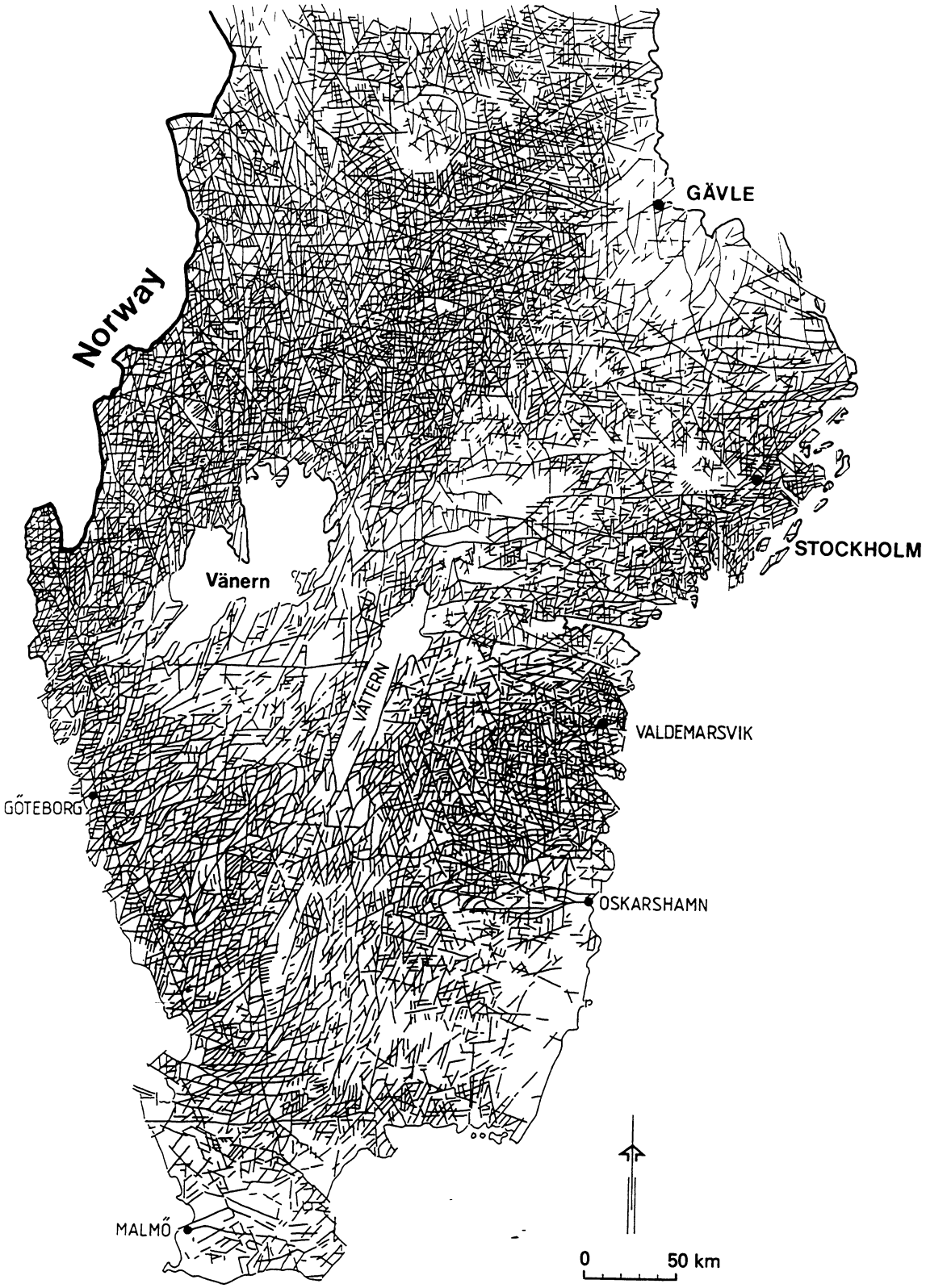

Figure 3 - Rock blocks and lineaments in southern Sweden interpreted from 1:2,000,000 relief maps (compiled from Tirén and Beckholmen, 1990, 1992).

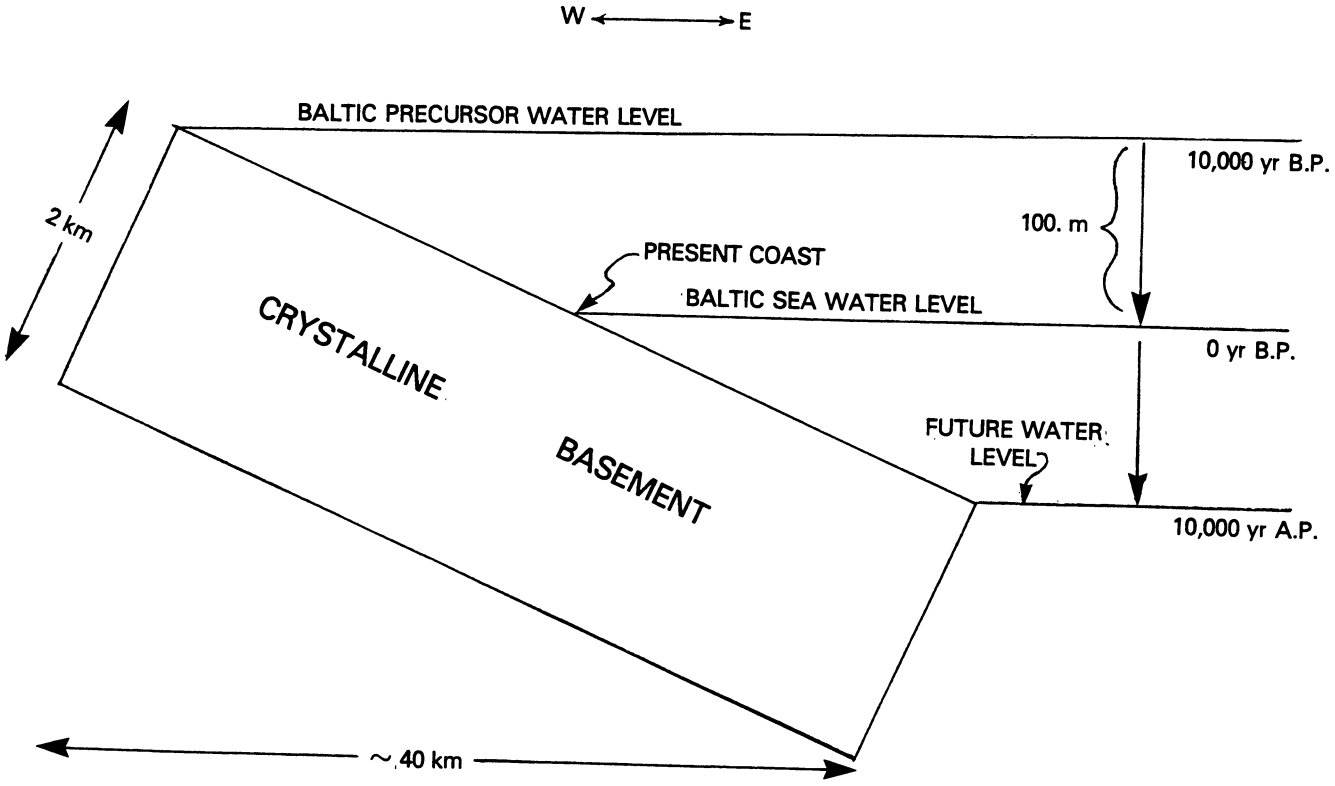

Figure 4 - Model section of crystalline basement centered on present east coast of central Sweden with typical surface dip and Holocene coastal regression.

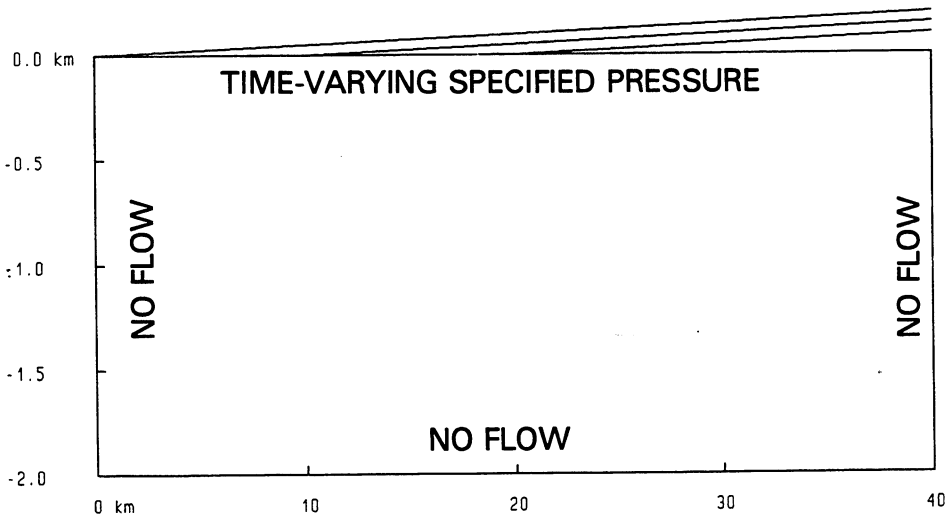

Figure 5 - Boundary conditions for regional simulations. Water level in Baltic Sea precursors used for time-varying specified pressure shown for 10000 yr B.P., 5000 yr B.P. and 0 yr B.P.

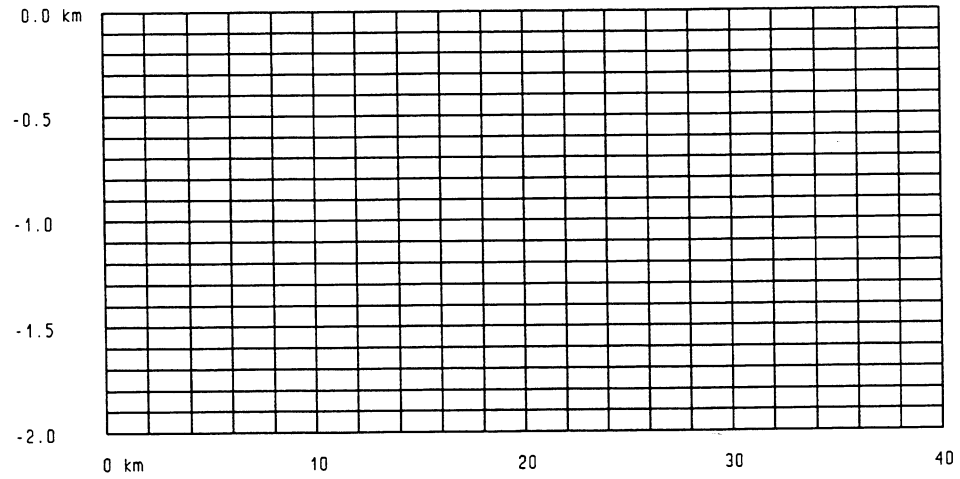

Figure 6 - Finite-element discretization for regional simulations. Mesh has 441 nodes and 400 elements. Each element is 2 km long and 100 m deep.

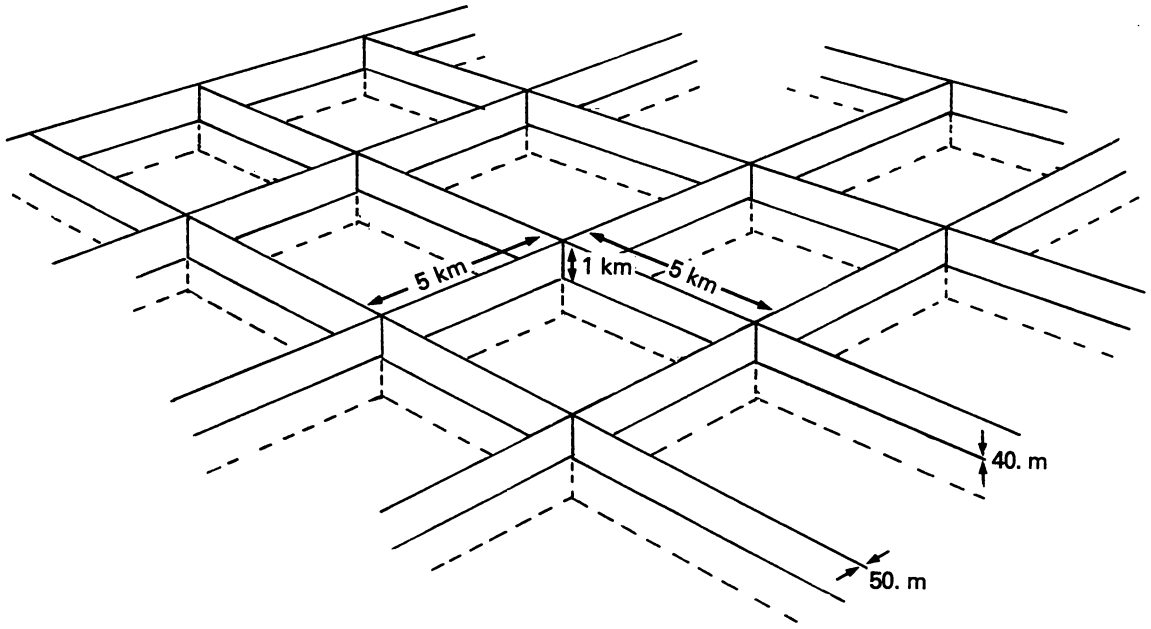

Figure 7 - Regional network of conductive zones used as a basis for the homogeneous models of the crystalline basement fabric.

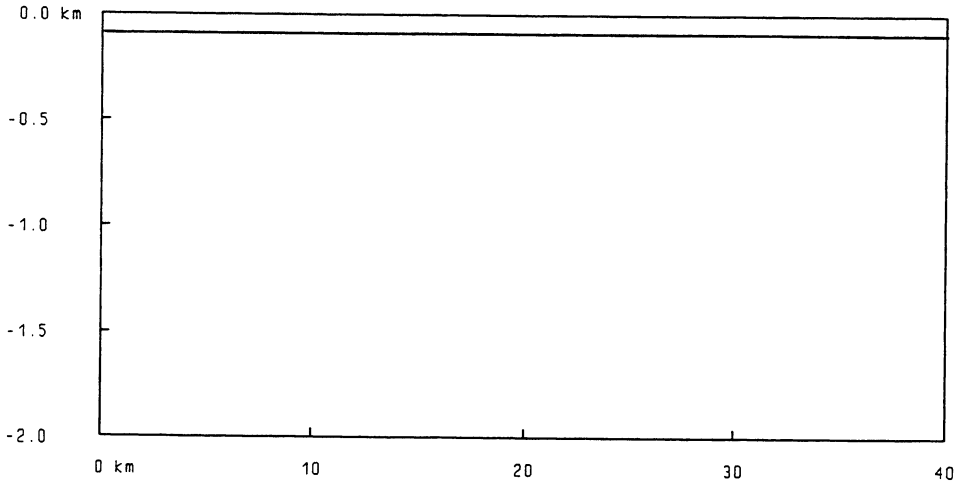

Figure 8a - Regional fabric: homogeneous model A with shallow 100 m thick conductive layer.

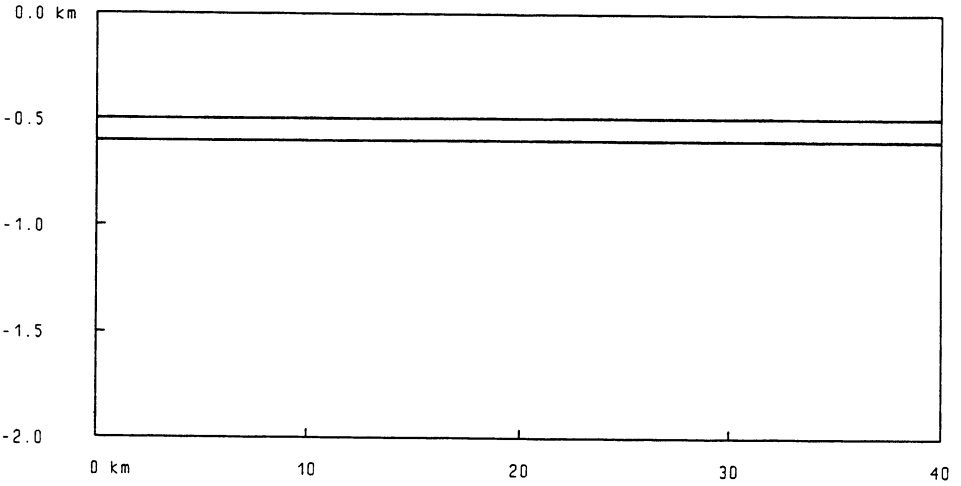

Figure 8b - Regional fabric: homogeneous model A with deep 100 m thick conductive layer.

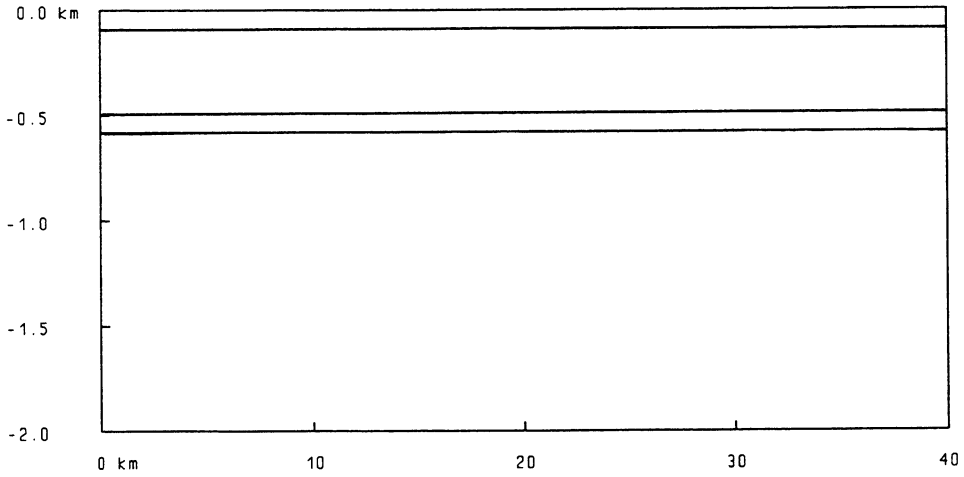

Figure 8c - Regional fabric: homogeneous model B with two shallow 100 m thick conductive layers.

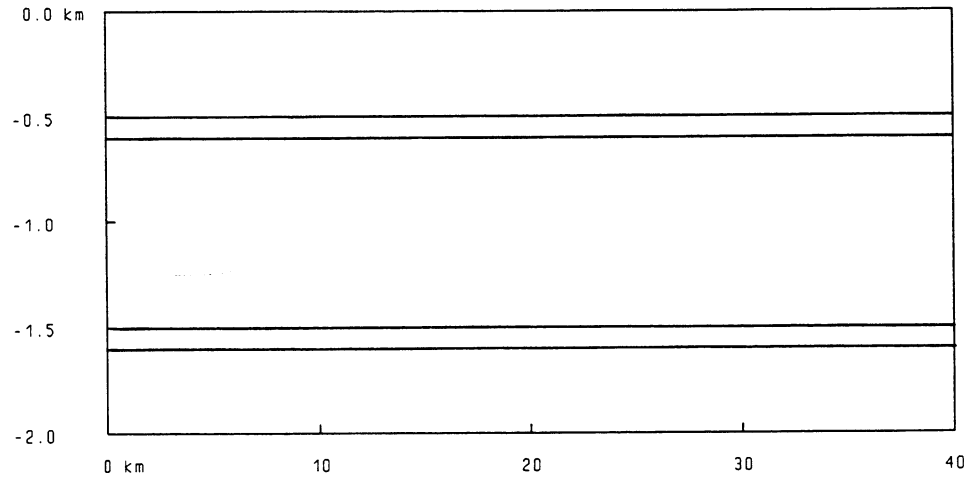

Figure 8d - Regional fabric: homogeneous model B with two deep 100 m thick conductive layers.

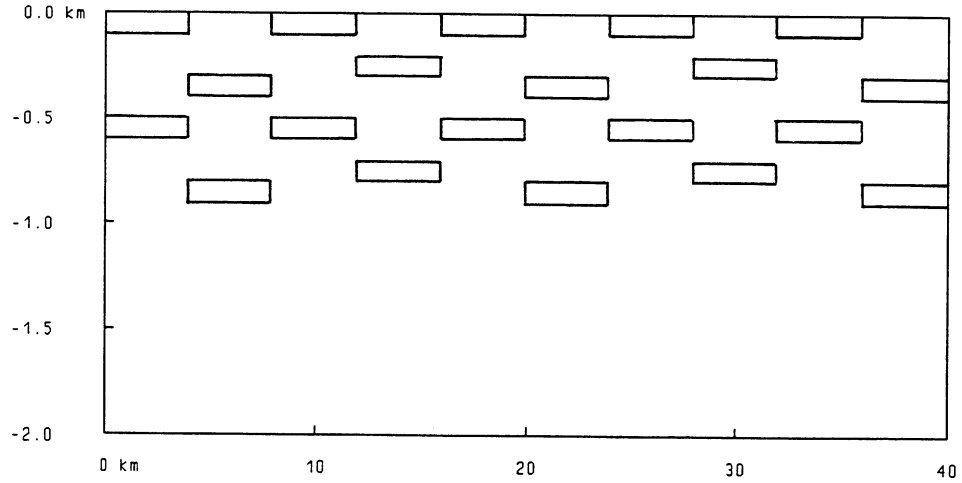

Figure 9 - Regional fabric: Homogeneous model B with two 100 m conductive layers offset by block faulting.

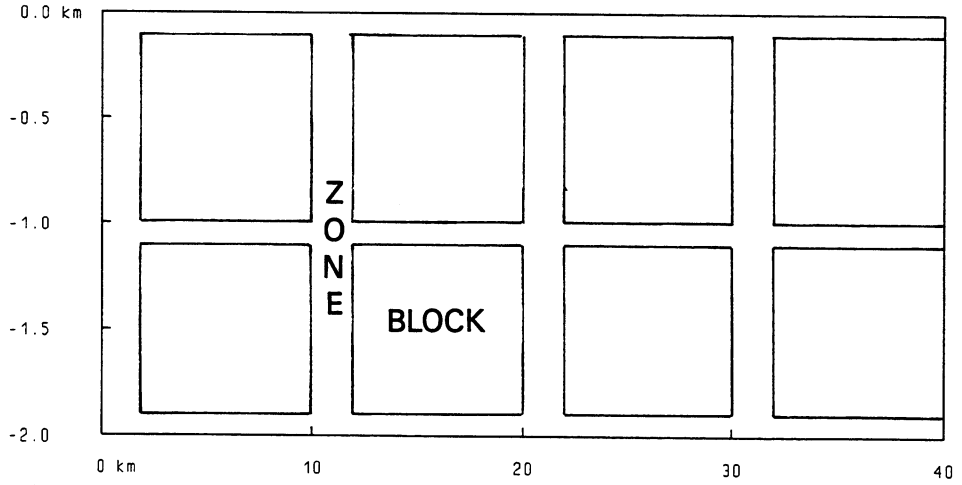

Figure 10 - Regional fabric: intersecting continuous conductive fracture zones.

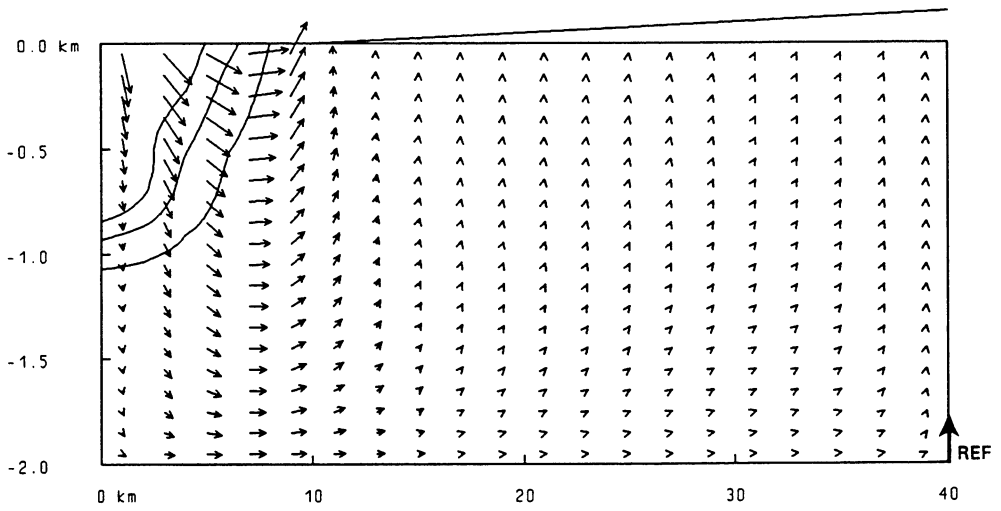

Figure 11a - Regional flow at 5000 yr B.P.: homogeneous model A. Isopachs indicate remaining old water at 15%, 50% and 85% of total fluid volume (from left to right). Reference velocity vector is $5x10^{-8}$ m/s.

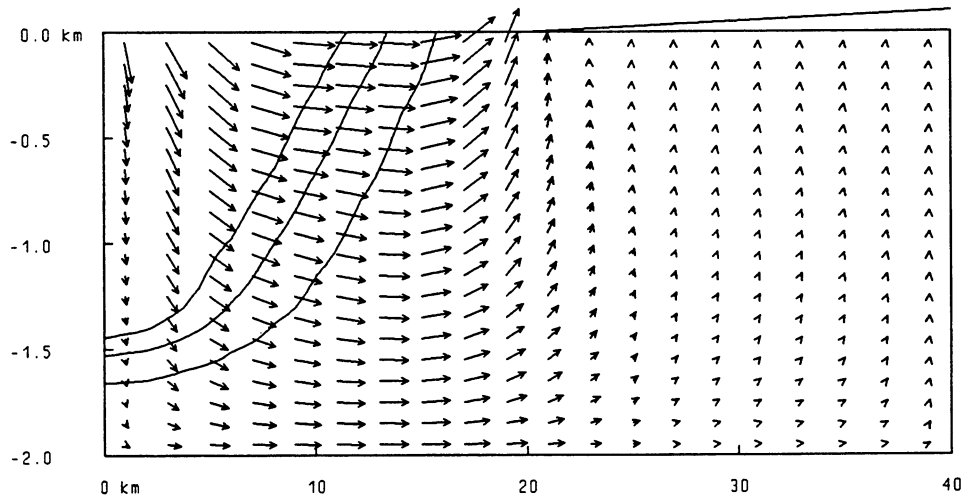

Figure 11b - Regional flow at present time (0 yr B.P.): homogeneous model A. Isopachs indicate remaining old water at 15%, 50% and 85% of total fluid volume (from left to right). Reference velocity vector is $5x10^{-8}$ m/s.

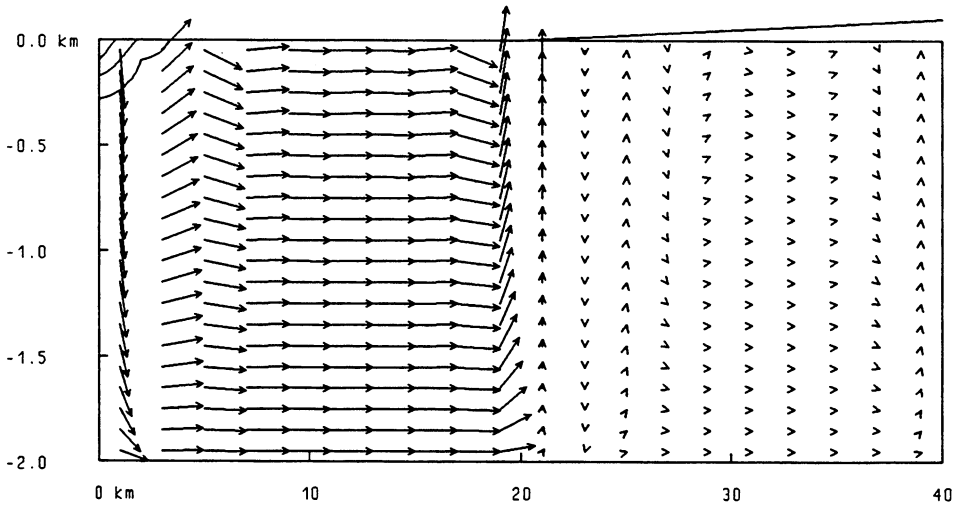

Figure 12 - Regional flow at present time (0 yr B.P.): homogeneous model B. Isopachs indicate remaining old water at 15%, 50% and 85% of total fluid volume (from left to right). Reference velocity vector is $5x10^{-10}$ m/s.

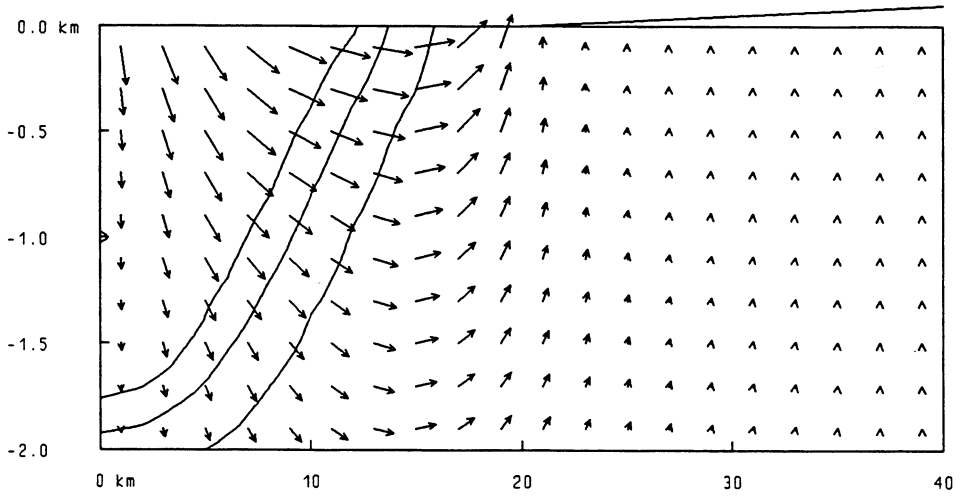

Figure 13 - Regional flow at present time (0 yr B.P.): homogeneous model A with depth of 4 km. Only upper half of section is shown.

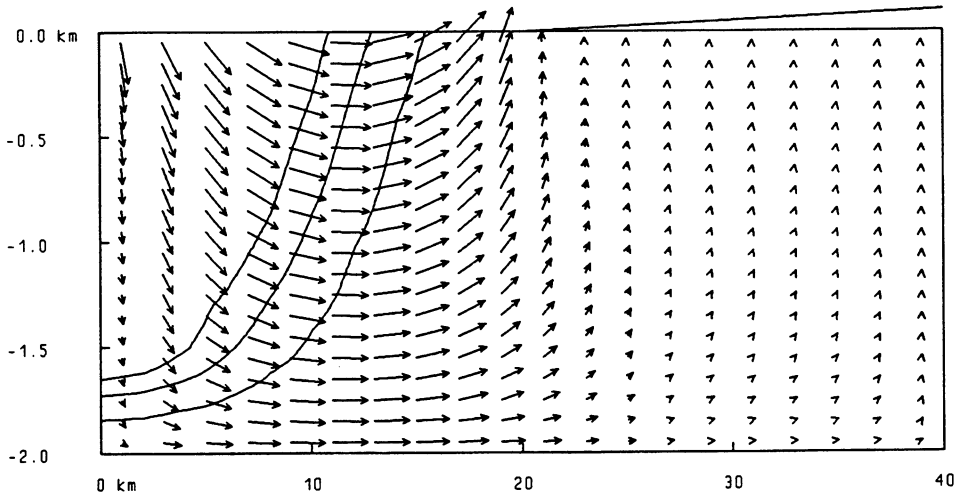

Figure 14 - Regional flow at present time (0 yr B.P.): homogeneous model A with constant fluid density. Isopachs (left to right, 15%, 50% and 85%) indicate volume of remaining old water. Reference velocity vector is $5x10^{-8}$ m/s.

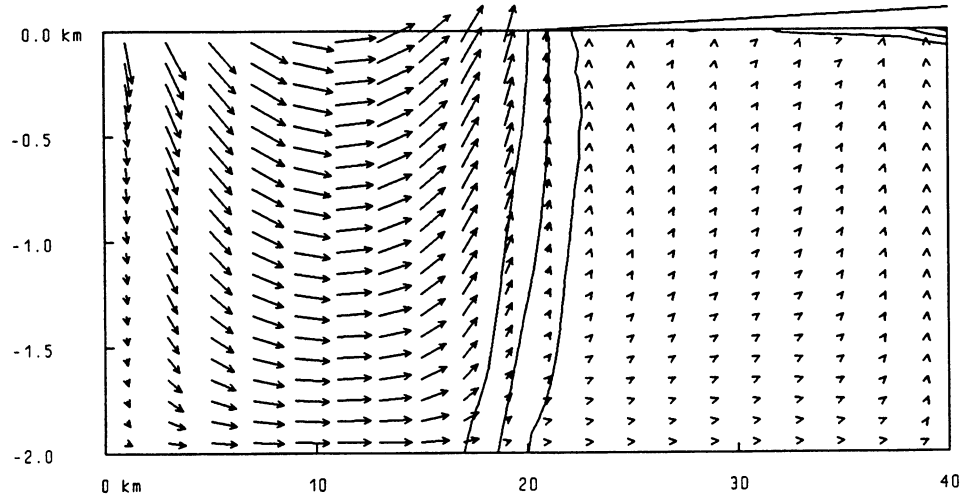

Figure 15 - Regional flow at present time (0 yr B.P.): homogeneous model A with reduced porosity of 10^{-4}. Isopachs (left to right, 15%, 50% and 85%) indicate volume of old water. Reference velocity vector is $5x10^{-7}$ m/s.

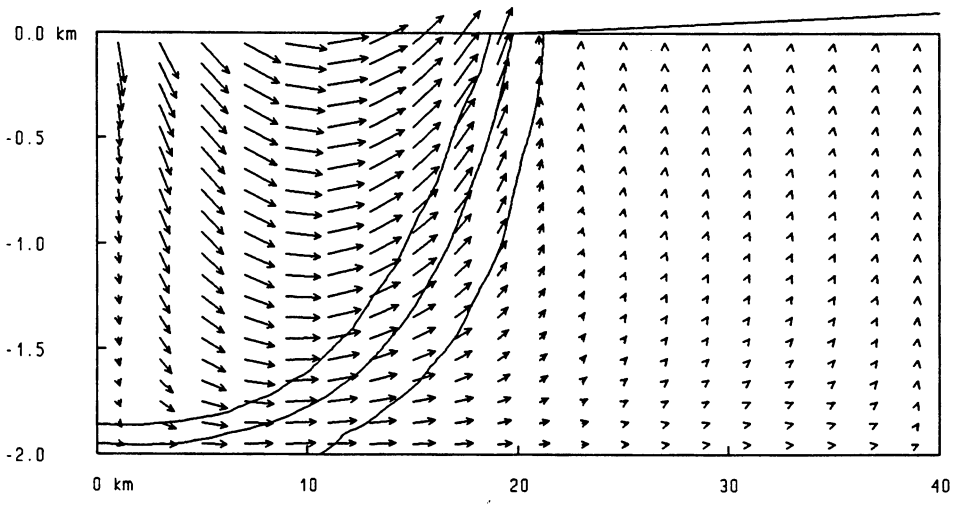

Figure 16a - Regional flow at 10000 yr A.P.: homogeneous model A with stationary coast. Isopachs (left to right, 15%, 50% and 85%) indicate volume of remaining old water. Reference velocity vector is $5x10^{-8}$ m/s.

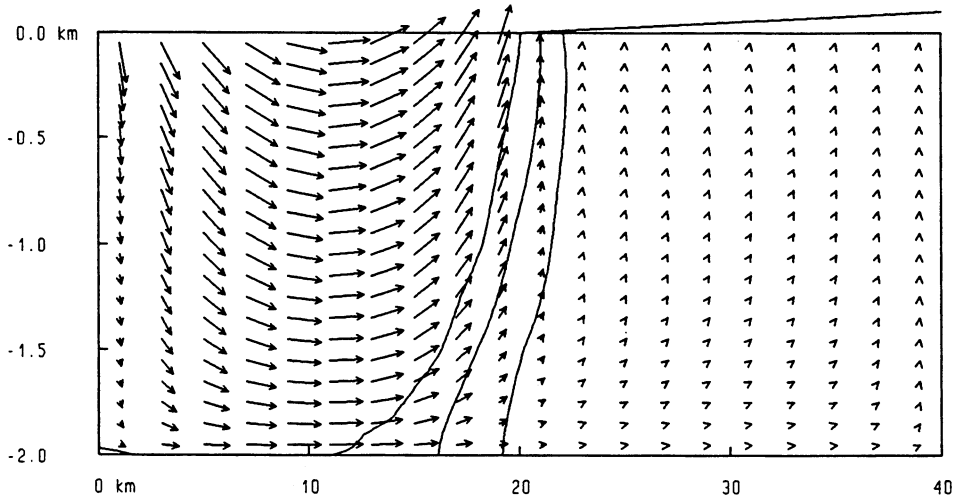

Figure 16b - Regional flow at 20000 yr A.P.: homogeneous model A with stationary coast. Isopachs (left to right, 15%, 50% and 85%) indicate volume of remaining old water. Reference velocity vector is $5x10^{-8}$ m/s.

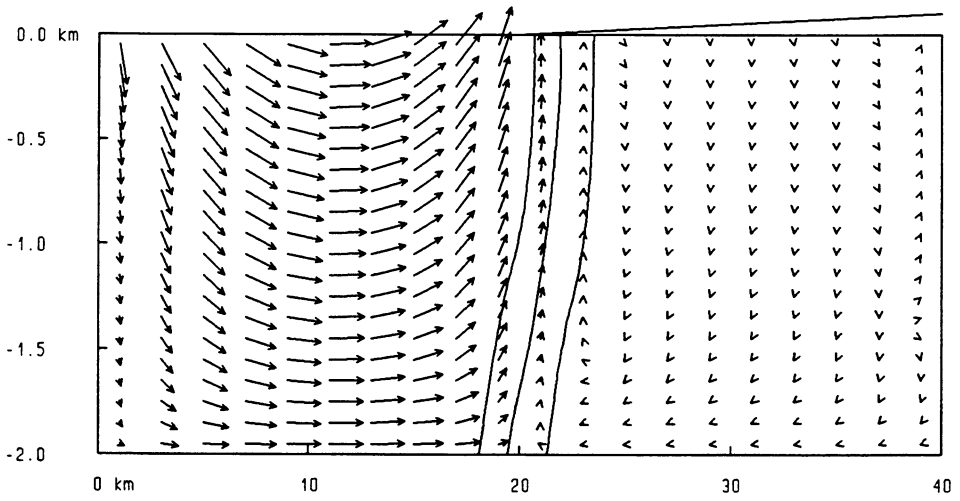

Figure 16c - Regional flow at 40000 yr A.P.: homogeneous model A with stationary coast. Isopachs (left to right, 15%, 50% and 85%) indicate volume of remaining old water. Reference velocity vector is $5x10^{-8}$ m/s.

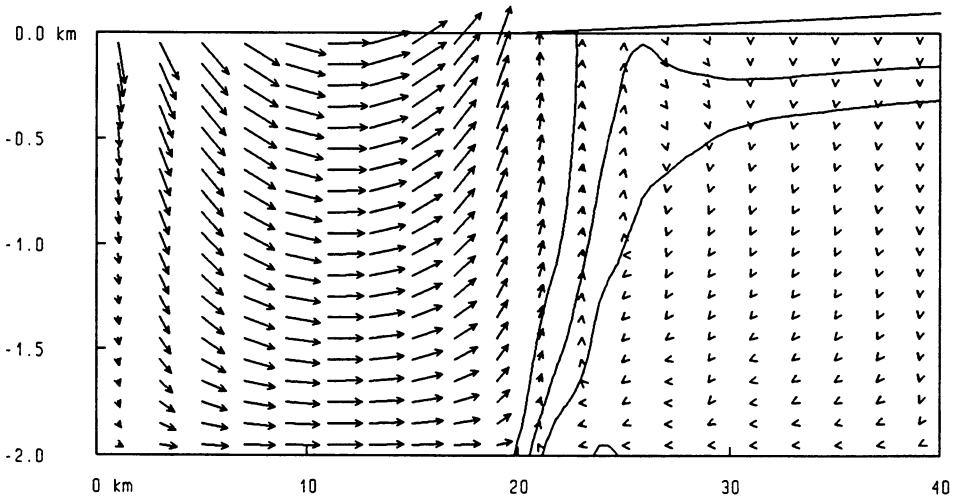

Figure 16d - Regional flow at 110000 yr A.P.: homogeneous model A with stationary coast. Isopachs (left to right, 15%, 50% and 85%) indicate volume of remaining old water. Reference velocity vector is $5x10^{-8}$ m/s.

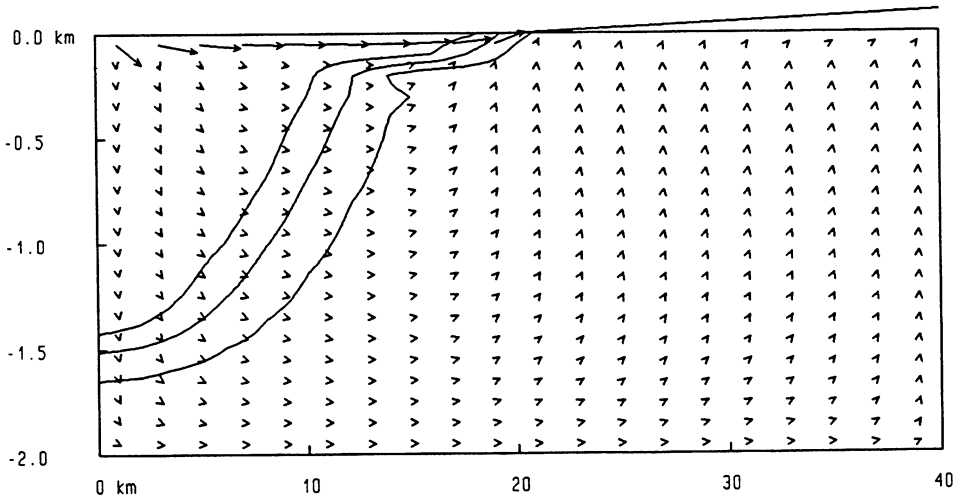

Figure 17 - Regional flow at present time (0 yr B.P.): homogeneous model A with shallow layer. Isopachs (left to right, 15%, 50% and 85%) indicate volume of remaining old water. Reference velocity vector is $5x10^{-7}$ m/s.

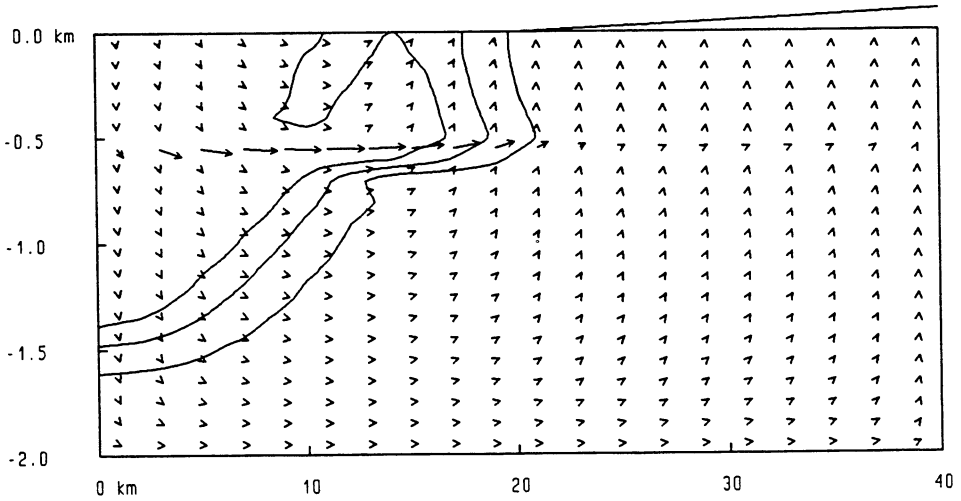

Figure 18 - Regional flow at present time (0 yr B.P.): homogeneous model A with deep layer. Isopachs (left to right, 15%, 50% and 85%) indicate volume of remaining old water. Reference velocity vector is $5x10^{-7}$ m/s.

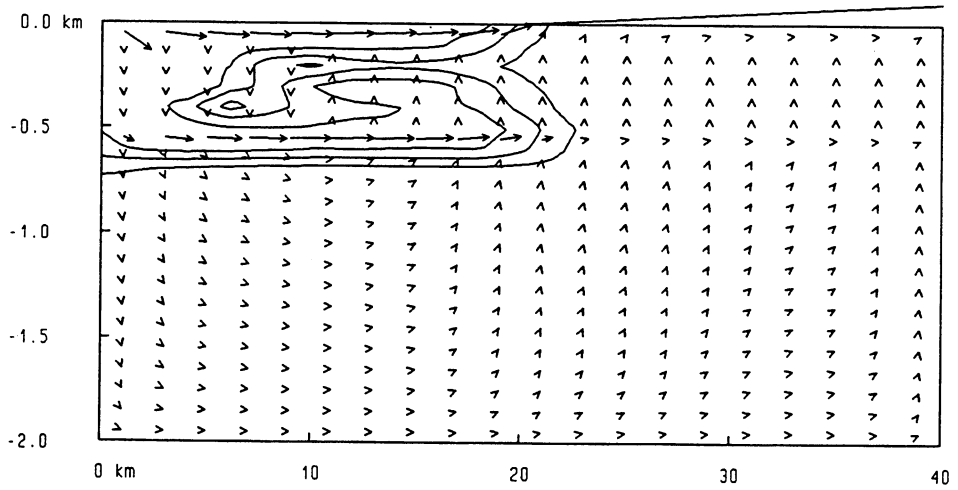

Figure 19 - Regional flow at present time (0 yr B.P.): homogeneous model B with two shallow layers. Isopachs (left to right, 15%, 50% and 85%) indicate volume of remaining old water. Reference velocity vector is $5x10^{-7}$ m/s.

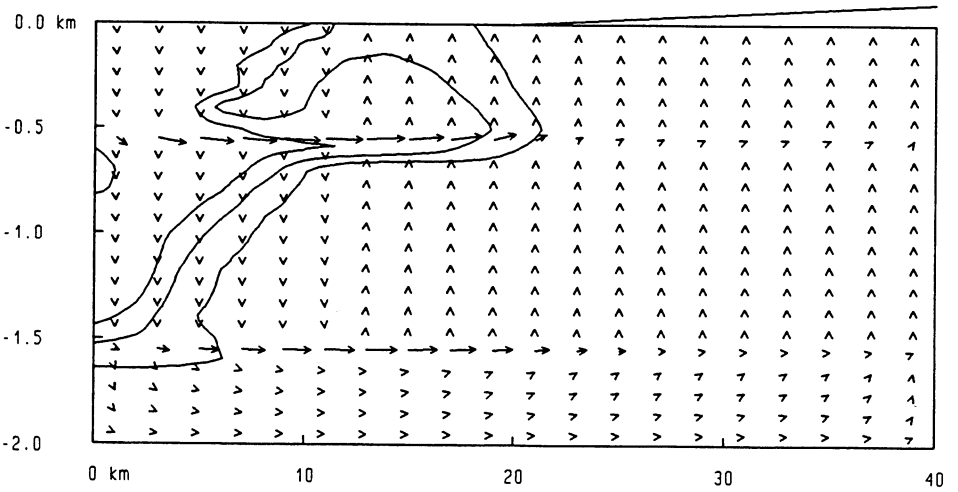

Figure 20 - Regional flow at present time (0 yr B.P.): homogeneous model B with two deep layers. Isopachs (left to right, 15%, 50% and 85%) indicate volume of remaining old water. Reference velocity vector is $5x10^{-7}$ m/s.

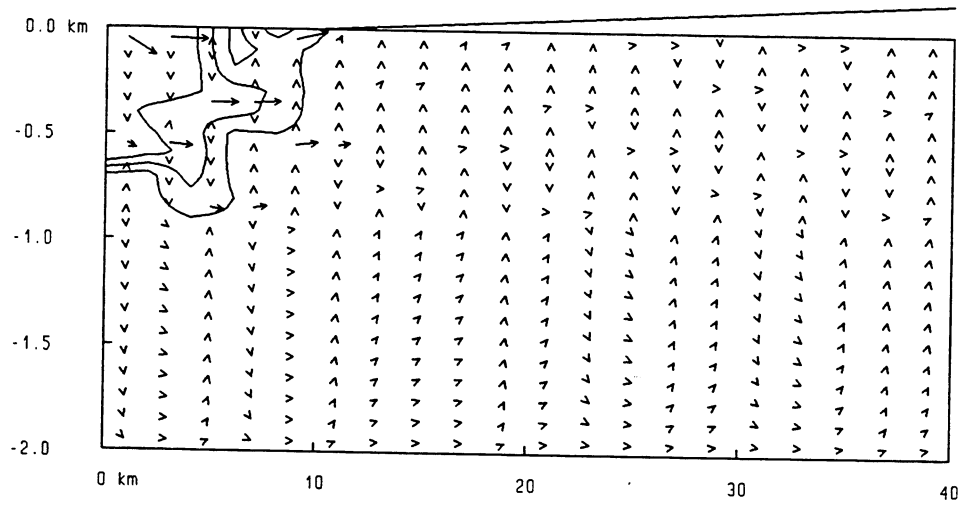

Figure 21a - Regional flow at 5000 yr B.P.: homogeneous model B with two layers and block faulting. Isopachs (left to right, 15%, 50% and 85%) indicate volume of remaining old water. Reference velocity vector is $5x10^{-7}$ m/s.

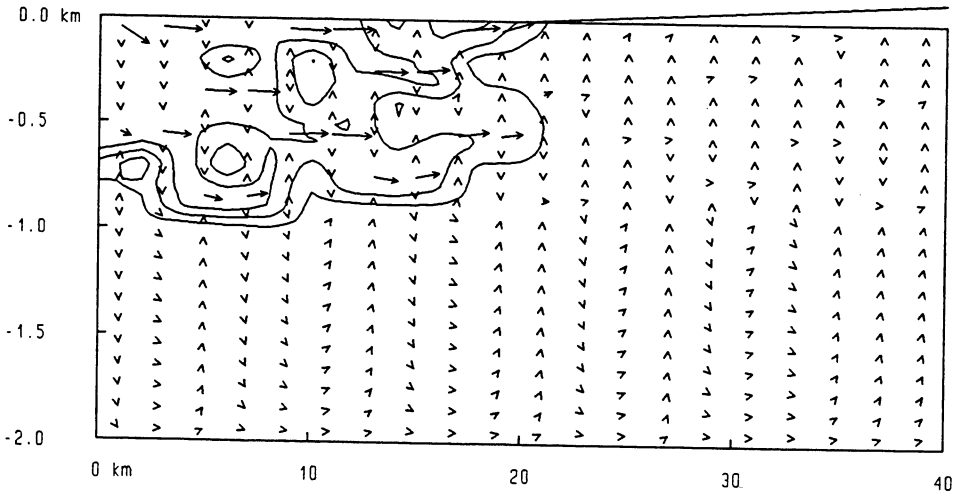

Figure 21b - Regional flow at present time (0 yr B.P.): homogeneous model B with two layers and block faulting. Isopachs (left to right, 15%, 50% and 85%) indicate volume of old water. Reference velocity vector is $5x10^{-7}$ m/s.

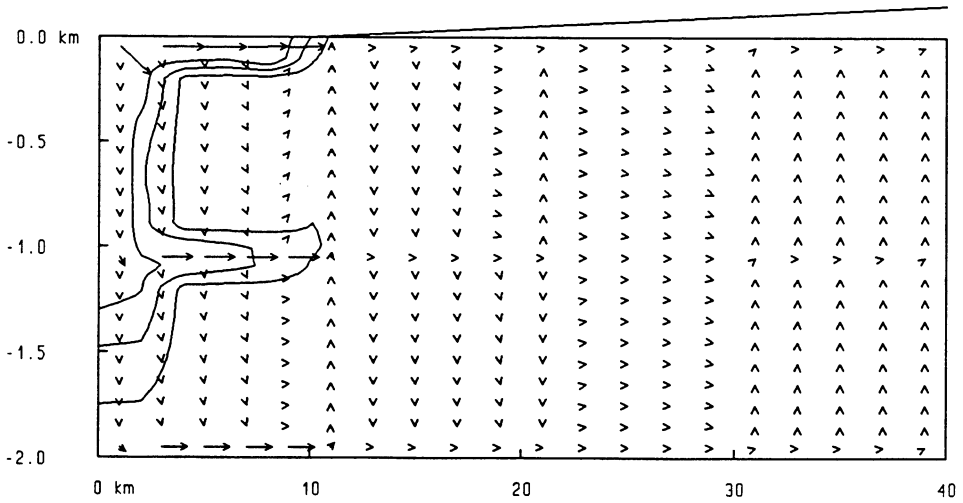

Figure 22a - Regional flow at 5000 yr B.P.: fabric with intersecting continuous fracture zones. Isopachs (left to right, 15%, 50% and 85%) indicate volume of remaining old water. Reference velocity vector is 5×10^{-7} m/s.

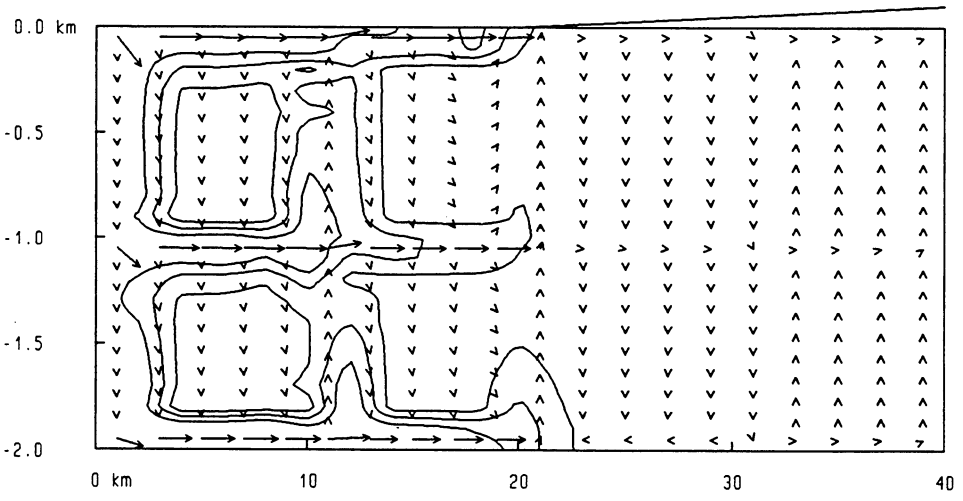

Figure 22b - Regional flow at present time (0 yr B.P.): intersecting fracture zone fabric (block conductivity, 10^{-10} m/s). Old water volume isopachs (left to right, 15%, 50%, 85%). Reference velocity, 5×10^{-7} m/s.

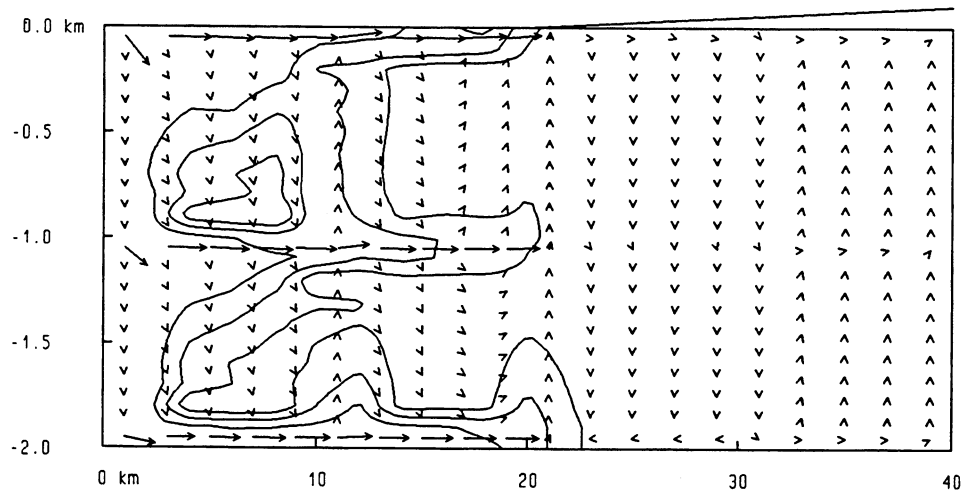

Figure 23 - Regional flow at present time (0 yr B.P.): intersecting fracture zone fabric (block conductivity, 10^{-9} m/s). Old water volume isopachs (left to right, 15%, 50%, 85%). Reference velocity, $5x10^{-7}$ m/s.

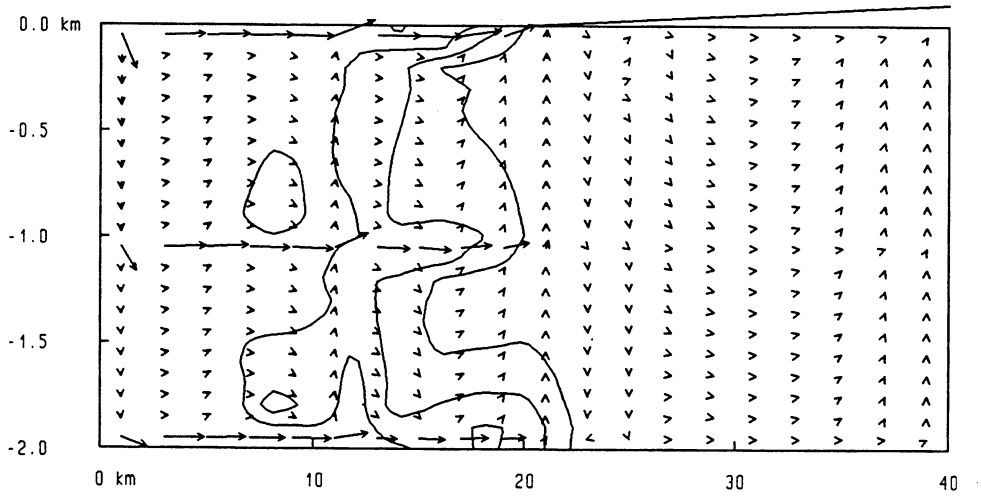

Figure 24 - Regional flow at present time (0 yr B.P.): intersecting fracture zone fabric (block conductivity, 10^{-8} m/s). Old water volume isopachs (left to right, 15%, 50%, 85%). Reference velocity, $5x10^{-7}$ m/s.

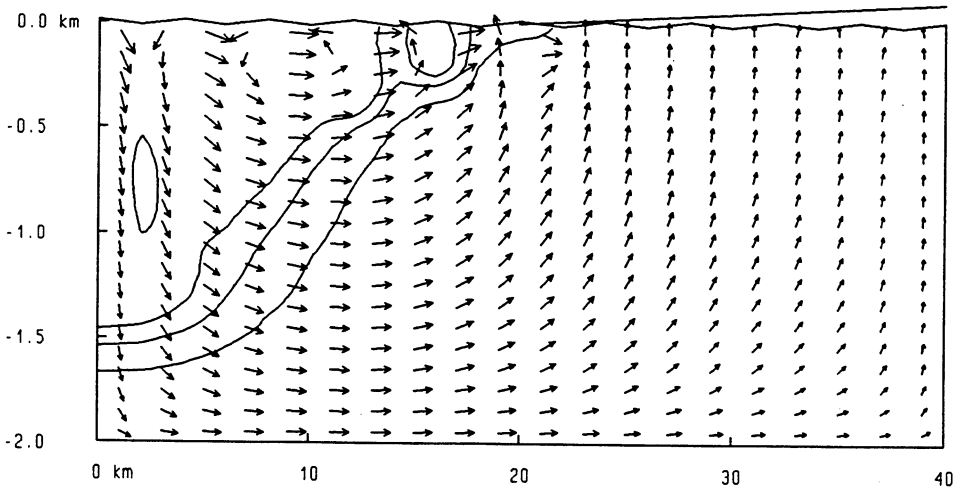

Figure 25 - Regional flow at present time (0 yr B.P.): homogeneous model A with surface relief of 25 m. Isopachs (left to right, 15%, 50% and 85%) indicate volume of remaining old water. Reference log-velocity vector is 5×10^{-7} m/s.

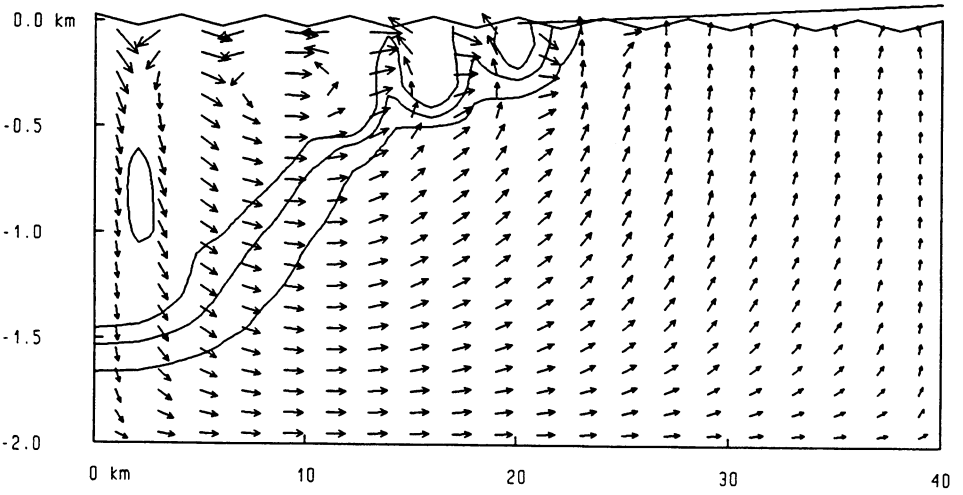

Figure 26 - Regional flow at present time (0 yr B.P.): homogeneous model A with surface relief of 50 m. Isopachs (left to right, 15%, 50% and 85%) indicate volume of remaining old water. Reference log-velocity vector is 5×10^{-7} m/s.

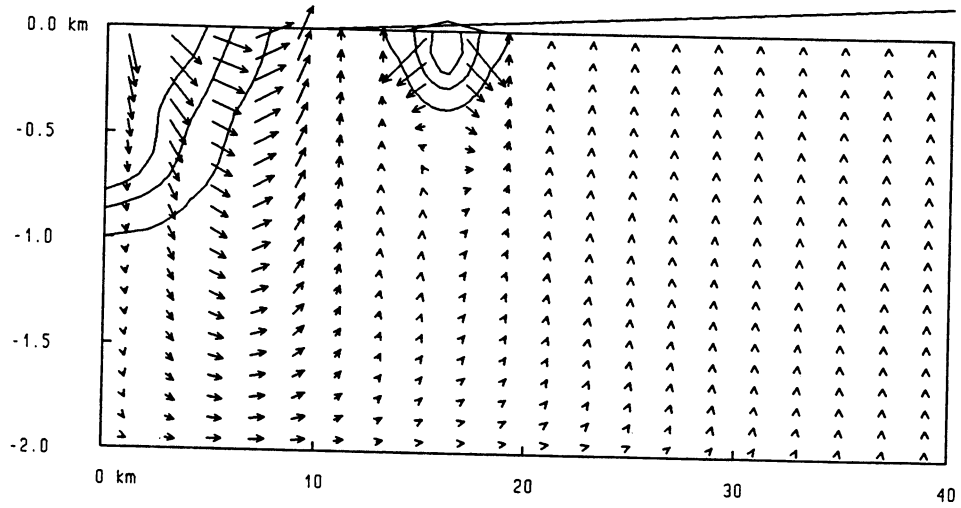

Figure 27a - Regional flow at 5000 yr B.P.: homogeneous model A with 50 m ridge. Isopachs (left to right, 15%, 50% and 85%) indicate volume of remaining old water. Reference velocity vector is $5x10^{-8}$ m/s.

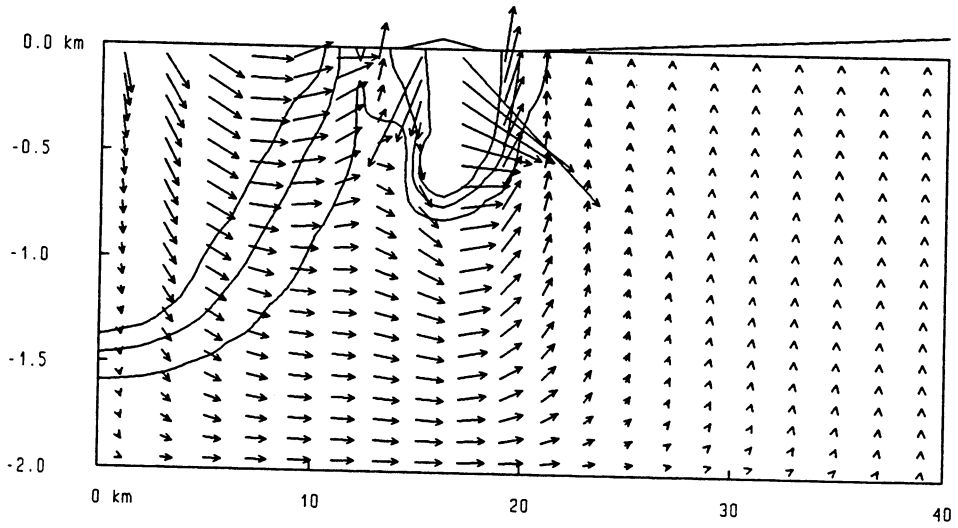

Figure 27b - Regional flow at present time (0 yr B.P.): homogeneous model A with 50 m ridge. Isopachs (left to right, 15%, 50% and 85%) indicate volume of remaining old water. Reference velocity vector is $5x10^{-8}$ m/s.

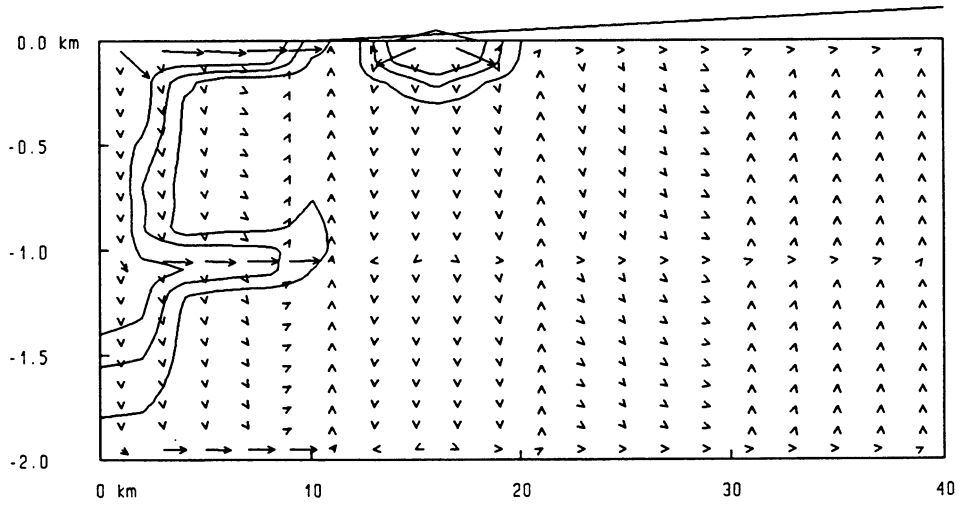

Figure 28a - Regional flow at 5000 yr B.P.: intersecting fracture zones (block conductivity, 10^{-9} m/s) with 50 m ridge. Old water volume isopachs (left to right, 15%, 50%, 85%). Reference velocity, $5x10^{-7}$ m/s.

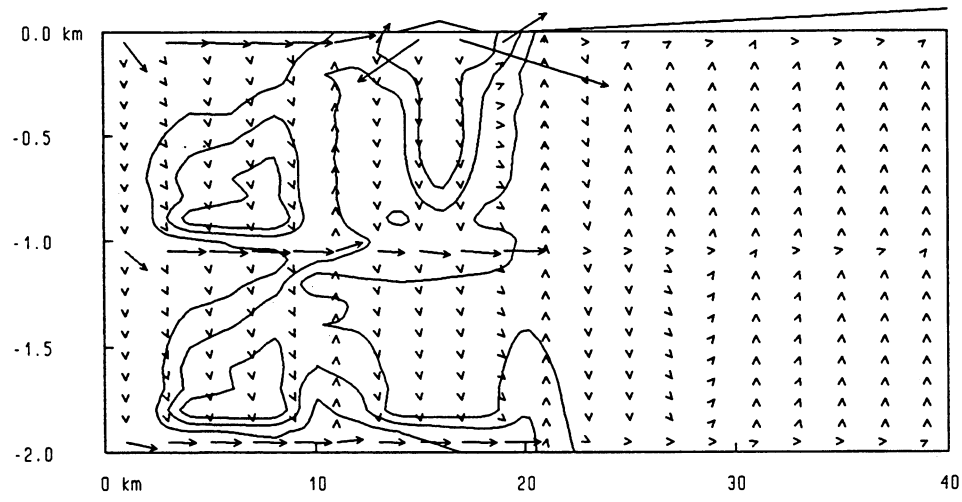

Figure 28b - Regional flow, present time (0 yr B.P.): intersecting fracture zones (block conductivity, 10^{-9} m/s), 50 m ridge. Old water volume isopachs (left-right, 15%, 50%, 85%). Reference velocity, $5x10^{-7}$ m/s.

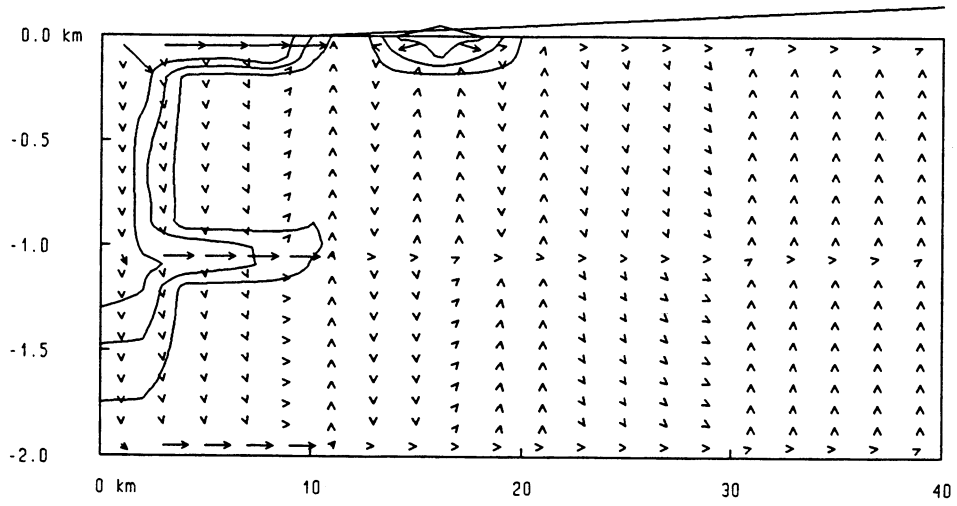

Figure 29a - Regional flow at 5000 yr B.P.: intersecting fracture zones (block conductivity, 10^{-10} m/s) with 50 m ridge. Old water volume isopachs (left to right, 15%, 50%, 85%). Reference velocity, $5x10^{-7}$ m/s.

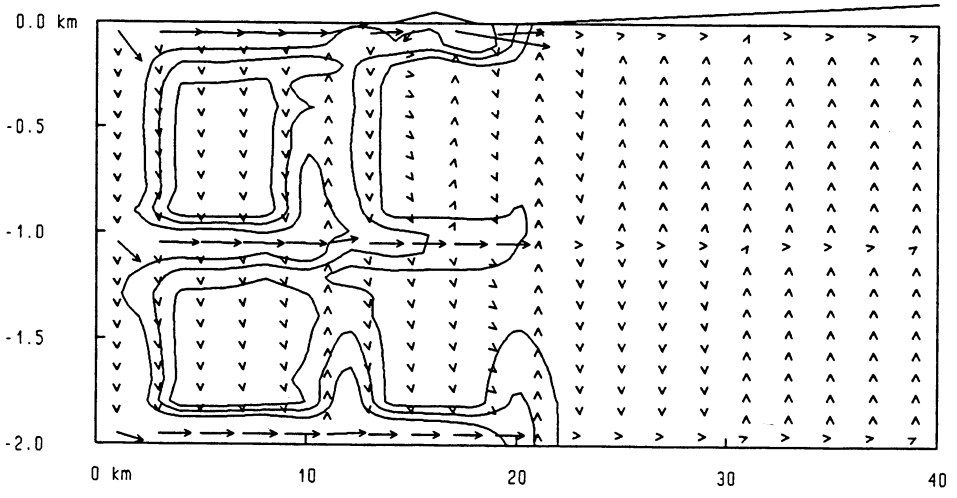

Figure 29b - Regional flow, present time (0 yr B.P.): intersecting fracture zones (block conductivity 10^{-10} m/s), 50 m ridge. Old water volume isopachs (left-right, 15%, 50%, 85%). Reference velocity, $5x10^{-7}$ m/s.

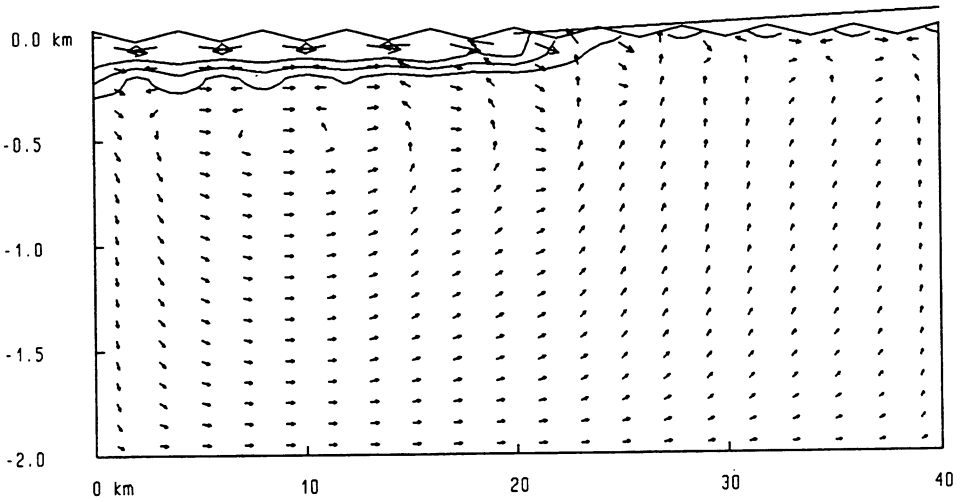

Figure 30 - Regional flow at present time (0 yr B.P.): homogeneous model A, 50 m relief, depth-dependent conductivity. Old water volume isopachs (left-right, 15%, 50%, 85%). Reference log-velocity, 5×10^{-7} m/s.

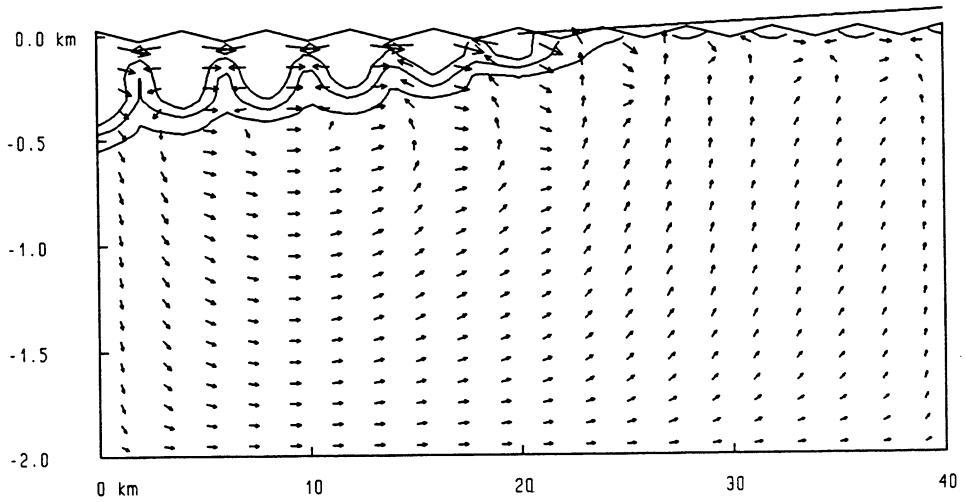

Figure 31 - Regional flow at present time (0 yr B.P.): homogeneous model A, 50 m relief, mild-depth-dependent conductivity. Old water volume isopachs (left-right, 15%, 50%, 85%). Reference log-velocity, 5×10^{-7} m/s.

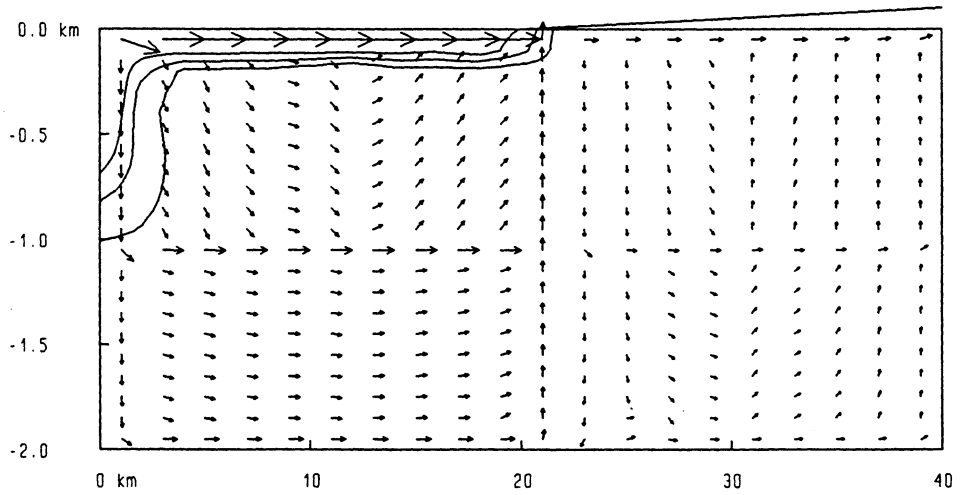

Figure 32 - Regional flow at present time (0 yr B.P.): intersecting fracture zones, depth-dependent conductivity (porosity 10^{-3}). Old water volume isopachs (left-right, 15%, 50%, 85%). Reference log-velocity, $5x10^{-7}$ m/s.

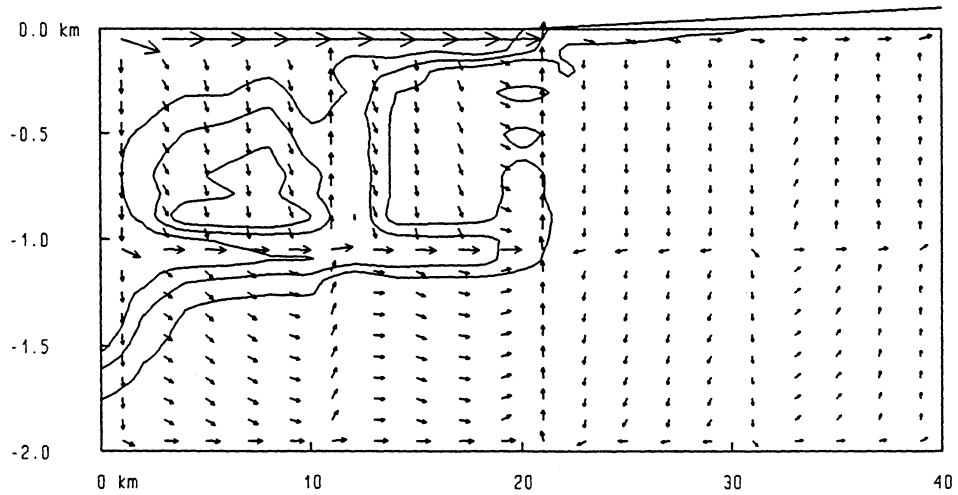

Figure 33 - Regional flow at present time (0 yr B.P.): intersecting fracture zones, depth-dependent conductivity (porosity 10^{-4}). Old water volume isopachs (left-right, 15%, 50%, 85%). Reference log-velocity, $5x10^{-6}$ m/s.

List of Figures

Figure 10 - Regional fabric: intersecting continuous conductive fracture zones.

Figure 11a - Regional flow at 5000 yr B.P.: homogeneous model A. Isopleths indicate remaining old water at 15%, 50% and 85% of total fluid volume (from left to right). Reference velocity vector is $5x10^{-8}$ m/s.

Figure 11b - Regional flow at present time (0 yr B.P.): homogeneous model A. Isopleths indicate remaining old water at 15%, 50% and 85% of total fluid volume (from left to right). Reference velocity vector is $5x10^{-8}$ m/s.

Figure 12 - Regional flow at present time (0 yr B.P.): homogeneous model B. Isopleths indicate remaining old water at 15%, 50% and 85% of total fluid volume (from left to right). Reference velocity vector is $5x10^{-10}$ m/s.

Figure 13 - Regional flow at present (0 yr B.P.): homogeneous model A with depth of 4 km. Only upper half of section is shown. Isopleths indicate remaining old water volume (left-right, 15%, 50% and 85%). Reference velocity vector is $5x10^{-8}$ m/s.

Figure 14 - Regional flow at present time (0 yr B.P.): homogeneous model A with constant fluid density. Isopleths (left to right, 15%, 50% and 85%) indicate volume of remaining old water. Reference velocity vector is $5x10^{-8}$ m/s.

Figure 15 - Regional flow at present time (0 yr B.P.): homogeneous model A with reduced porosity of 10^{-4}. Isopleths (left to right, 15%, 50% and 85%) indicate volume of old water. Reference velocity vector is $5x10^{-7}$ m/s.

Figure 16a - Regional flow at 10000 yr A.P.: homogeneous model A with stationary coast. Isopleths (left to right, 15%, 50% and 85%) indicate volume of remaining old water. Reference velocity vector is $5x10^{-8}$ m/s.

Figure 16b - Regional flow at 20000 yr A.P.: homogeneous model A with stationary coast. Isopleths (left to right, 15%, 50% and 85%) indicate volume of remaining old water. Reference velocity vector is $5x10^{-8}$ m/s.

Figure 16c - Regional flow at 40000 yr A.P.: homogeneous model A with stationary coast. Isopleths (left to right, 15%, 50% and 85%) indicate volume of remaining old water. Reference velocity vector is $5x10^{-8}$ m/s.

Figure 16d - Regional flow at 110000 yr A.P.: homogeneous model A with stationary coast. Isopleths (left to right, 15%, 50% and 85%) indicate volume of remaining old water. Reference velocity vector is $5x10^{-8}$ m/s.

Figure 17 - Regional flow at present time (0 yr B.P.): homogeneous model A with shallow layer (Figure 8a). Isopleths (left to right, 15%, 50% and 85%) indicate volume of remaining old water. Reference velocity vector is $5x10^{-7}$ m/s.

Figure 18 - Regional flow at present time (0 yr B.P.): homogeneous model A with deep layer (Figure 8b). Isopleths (left to right, 15%, 50% and 85%) indicate volume of remaining old water. Reference velocity vector is $5x10^{-7}$ m/s.

Figure 19 - Regional flow at present time (0 yr B.P.): homogeneous model B with two shallow layers (Figure 8c). Isopleths (left to right, 15%, 50% and 85%) indicate volume of remaining old water. Reference velocity vector is $5x10^{-7}$ m/s.

Figure 20 - Regional flow at present time (0 yr B.P.): homogeneous model B with two deep layers (Figure 8d). Isopleths (left to right, 15%, 50% and 85%) indicate volume of remaining old water. Reference velocity vector is $5x10^{-7}$ m/s.

Figure 21a - Regional flow at 5000 yr B.P.: homogeneous model B with two layers and block faulting (Figure 9). Isopleths (left-right, 15%, 50% and 85%) indicate volume of remaining old water. Reference velocity vector is $5x10^{-7}$ m/s.

Figure 21b - Regional flow at present time (0 yr B.P.): homogeneous model B with two layers and block faulting (Figure 9). Isopleths (left to right, 15%, 50% and 85%) show volume of old water. Reference velocity vector is $5x10^{-7}$ m/s.

Figure 22a - Regional flow at 5000 yr B.P.: fabric with intersecting continuous fracture zones (Figure 10). Isopleths (left to right, 15%, 50% and 85%) show volume of remaining old water. Reference velocity vector is $5x10^{-7}$ m/s.

Figure 22b - Regional flow at present (0 yr B.P.): intersecting fracture zone fabric (block conductivity, 10^{-10} m/s). Old water volume isopleths (left to right, 15%, 50%, 85%). Reference velocity, $5x10^{-7}$ m/s.

Figure 23 - Regional flow at present (0 yr B.P.): intersecting fracture zone fabric (Figure 10)(block conductivity, 10^{-9} m/s). Old water volume isopleths (left to right, 15%, 50%, 85%). Reference velocity, $5x10^{-7}$ m/s.

Figure 24 - Regional flow at present (0 yr B.P.): intersecting fracture zone fabric (Figure 10)(block conductivity, 10^{-8} m/s). Old water volume isopleths (left to right, 15%, 50%, 85%). Reference velocity, $5x10^{-7}$ m/s.

Figure 25 - Regional flow at present time (0 yr B.P.): homogeneous model A with surface relief of 25 m. Isopleths (left to right, 15%, 50% and 85%) indicate volume of remaining old water. Reference log-velocity vector is $5x10^{-7}$ m/s.

Figure 26 - Regional flow at present time (0 yr B.P.): homogeneous model A with surface relief of 50 m. Isopleths (left to right, 15%, 50% and 85%) indicate volume of remaining old water. Reference log-velocity vector is $5x10^{-7}$ m/s.

Figure 27a - Regional flow at 5000 yr B.P.: homogeneous model A with 50 m ridge. Isopleths (left to right, 15%, 50% and 85%) indicate volume of remaining old water. Reference velocity vector is $5x10^{-8}$ m/s.

Figure 27b - Regional flow at present time (0 yr B.P.): homogeneous model A with 50 m ridge. Isopleths (left to right, 15%, 50% and 85%) indicate volume of remaining old water. Reference velocity vector is $5x10^{-8}$ m/s.

Figure 28a - Regional flow at 5000 yr B.P.: intersecting fracture zones (Figure 10)(block conductivity, 10^{-9} m/s) with 50 m ridge. Old water isopleths (left to right, 15%, 50%, 85%). Ref. velocity, $5x10^{-7}$ m/s.

Figure 28b - Regional flow, at present (0 yr B.P.): intersecting fracture zones (Figure 10)(block conductivity, 10^{-9} m/s), 50 m ridge. Old water isopleths (left-right, 15%, 50%, 85%). Ref. velocity, $5x10^{-7}$ m/s.

Figure 29a - Regional flow, 5000 yr B.P.: intersecting fracture zones (Figure 10)(block conductivity, 10^{-10} m/s) with 50 m ridge. Old water volume isopleths (left-right, 15%, 50%, 85%). Ref. velocity, $5x10^{-7}$ m/s.

Figure 29b - Regional flow, present (0 yr B.P.): intersecting fracture zones (Figure 10)(block conductivity 10^{-10} m/s), 50 m ridge. Old water isopleths (left-right, 15%, 50%, 85%). Ref. velocity, $5x10^{-7}$ m/s.

Figure 30 - Regional flow at present time (0 yr B.P.): homogeneous model A, 50 m relief, depth-dependent conductivity. Old water volume isopleths (left-right, 15%, 50%, 85%). Reference log-velocity, $5x10^{-7}$ m/s.

Figure 31 - Regional flow at present time (0 yr B.P.): homogeneous model A, 50 m relief, mild-depth-dependent conductivity. Old water volume isopleths (left-right, 15%, 50%, 85%). Reference log-velocity, $5x10^{-7}$ m/s.

Figure 32 - Regional flow at present time (0 yr B.P.): intersecting fracture zones, depth-dependent conductivity (porosity 10^{-3}). Old water volume isopleths (left-right, 15%, 50%, 85%). Reference log-velocity, $5x10^{-7}$ m/s.

Figure 33 - Regional flow at present time (0 yr B.P.): intersecting fracture zones, depth-dependent conductivity (porosity 10^{-4}). Old water volume isopleths (left-right, 15%, 50%, 85%). Reference log-velocity, $5x10^{-6}$ m/s.

www.ski.se

STATENS KÄRNKRAFTINSPEKTION
Swedish Nuclear Power Inspectorate

POST/POSTAL ADDRESS SE-106 58 Stockholm
BESÖK/OFFICE Klarabergsviadukten 90
TELEFON/TELEPHONE +46 (0)8 698 84 00
TELEFAX +46 (0)8 661 90 86
E-POST/E-MAIL ski@ski.se
WEBBPLATS/WEB SITE www.ski.se